Searching for Inflationary Gravitational Waves in CMB polarization: from Planck to B-mode experiments

Carlo Baccigalupi (SISSA)

Cosmology 2018

Dubrovnik, October 25th, 2018

Outline

- Cosmological sources of B-modes in CMB Polarization Anisotropies
- Status of observations & Challenges
- B-mode experiments in the next decade

Outline

- Cosmological sources of B-modes in CMB Polarization Anisotropies
  - Primordial gravitational waves
  - Dark Energy
- Status of observations & Challenges
  - Planck 2018
  - B-mode probes
  - Ongoing challenges
- B-mode experiments in the next decade

Cosmological Sources of B-modes in CMB Polarization Anisotropies

CMB angular power spectrum

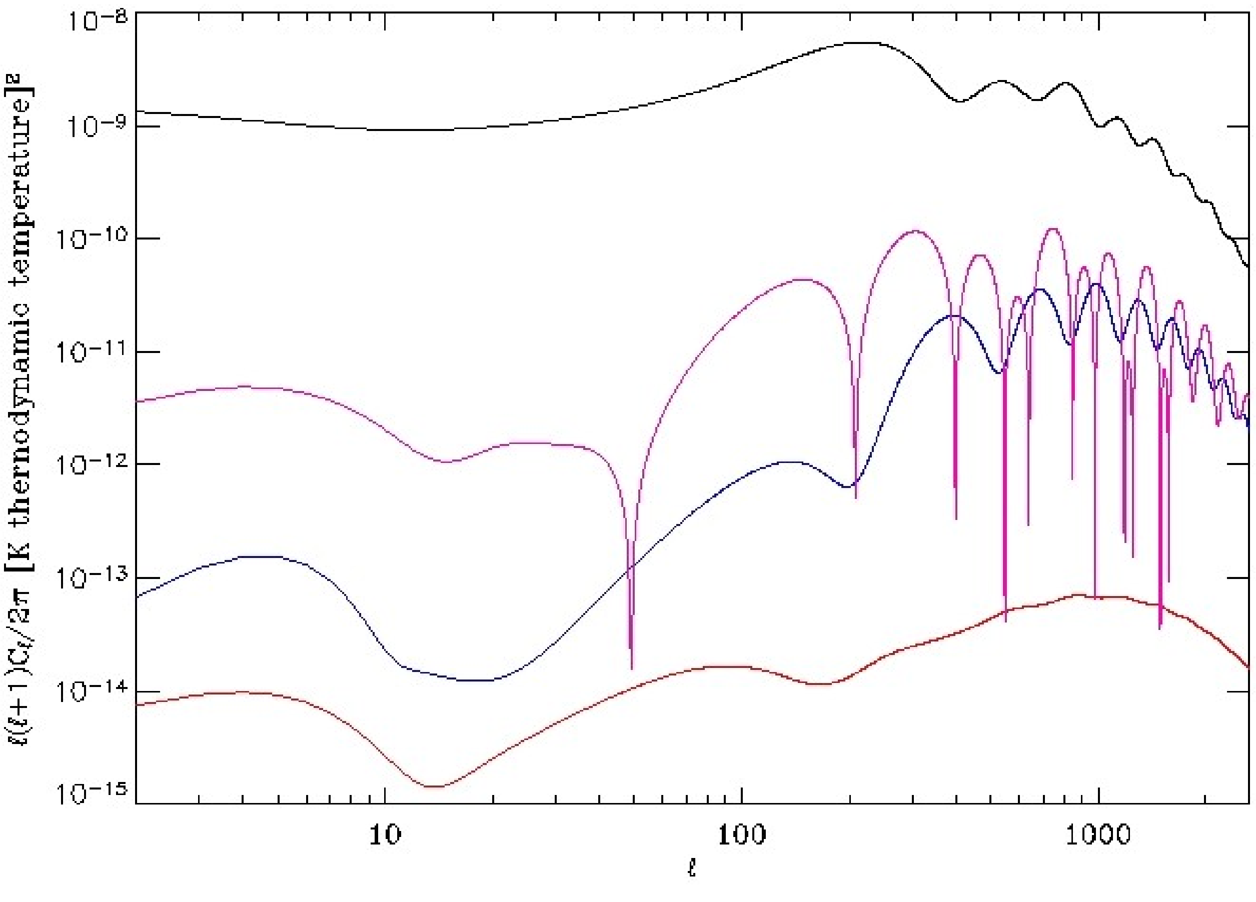

Angle ≈ 200/l degrees

CMB physics: Boltzmann equation

$$\frac{d\ \text{photons}}{dt} = \text{gravity} + \text{Compton scattering}$$

$$\frac{d\ \text{baryons+leptons}}{dt} = \text{gravity} + \text{Compton scattering}$$

CMB physics: Boltzmann equation

$$\frac{d\ \text{neutrinos}}{dt} = \text{gravity} + \text{weak interaction}$$

$$\frac{d\ \text{dark matter}}{dt} = \text{gravity} + \text{weak interaction (?)}$$

CMB physics: Boltzmann equation

$$\frac{d\,\text{neutrinos}}{dt} = \text{gravity} + \text{weak interaction}$$

$$\frac{d\,\text{dark matter}}{dt} = \text{gravity} + \text{weak interaction (?)}$$

gravity = photons + neutrinos + baryons + leptons + dark matter

CMB physics: gravity

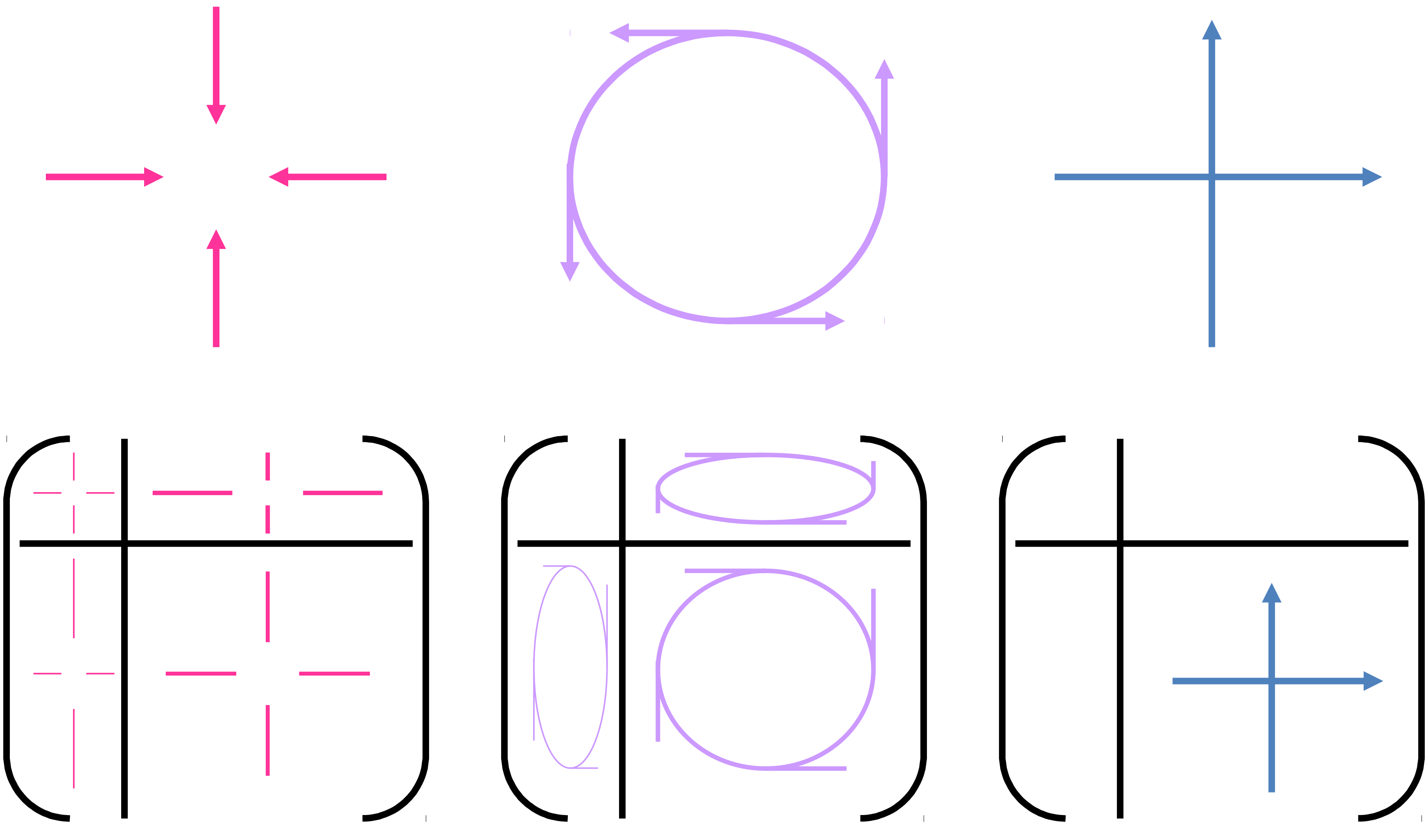

CMB physics: gravity

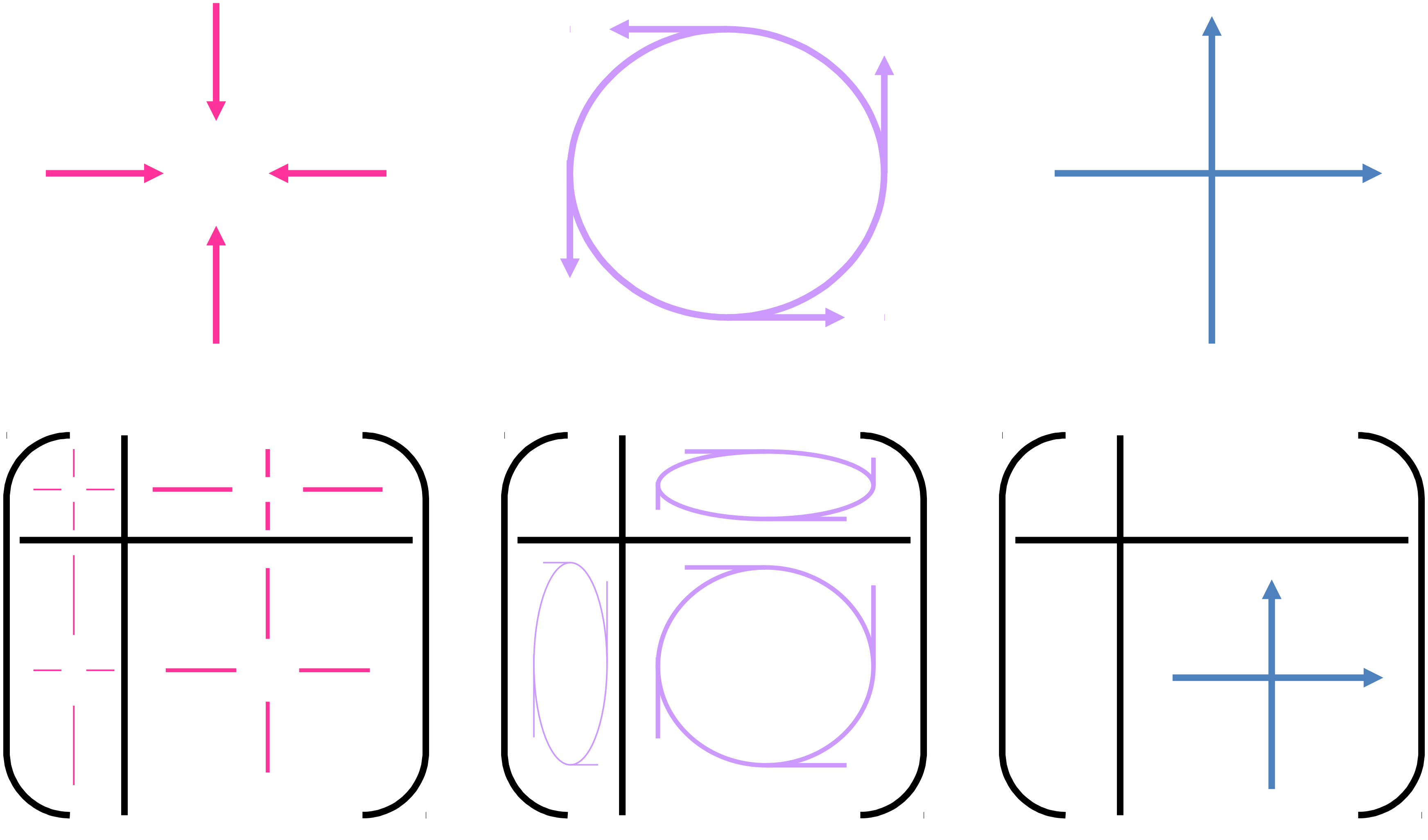

CMB Physics: Compton scattering

- Compton scattering is anisotropic
- An anisotropic incident intensity determines a linear polarization in the outgoing radiation
- At decoupling that happens due to the finite width of last scattering and the cosmological local quadrupole

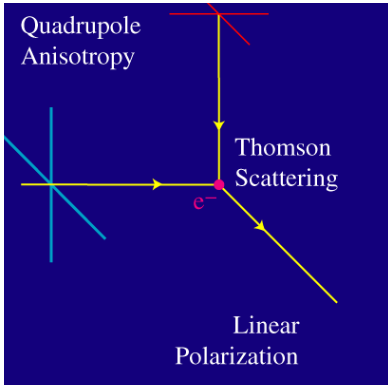

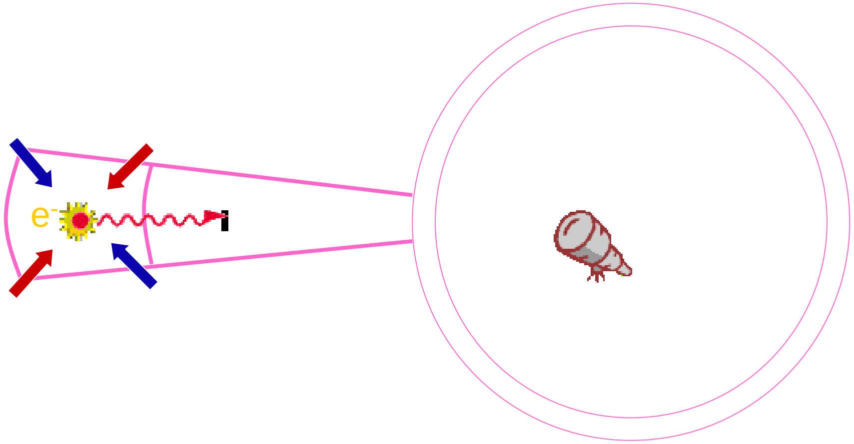

CMB anisotropy: Total Intensity

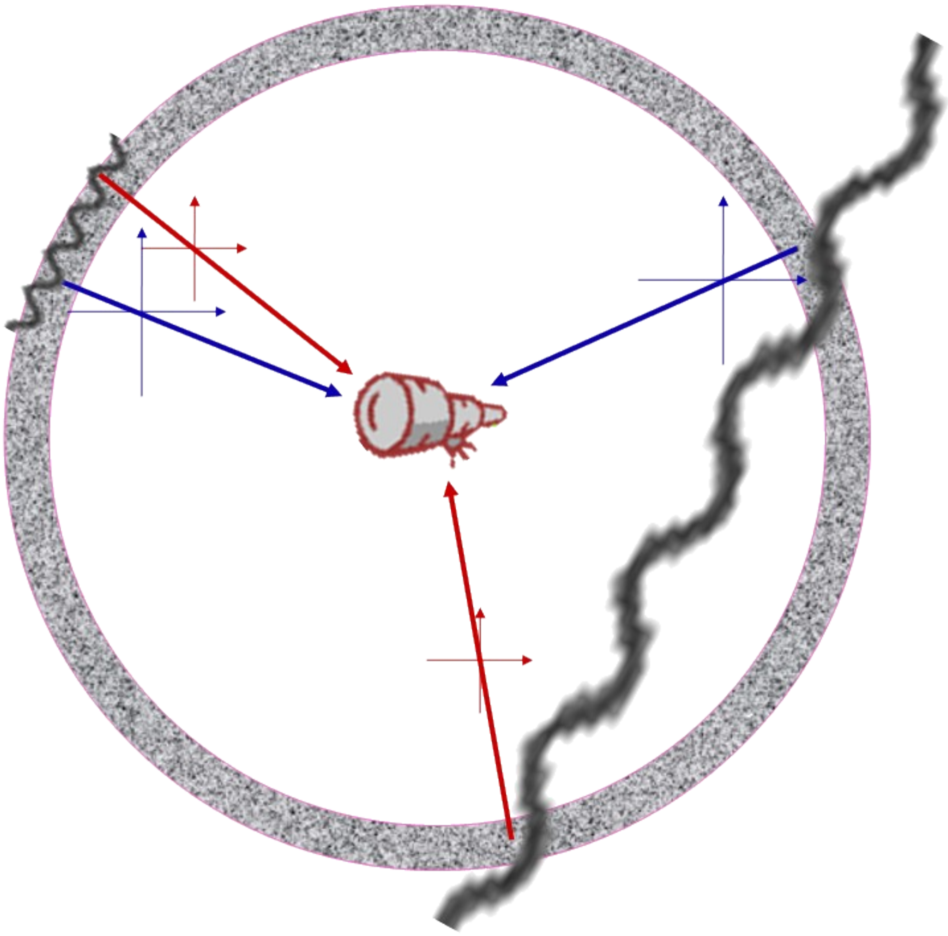

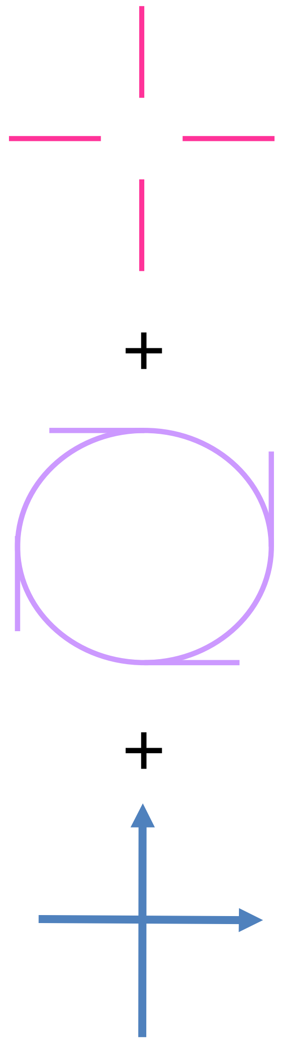

CMB anisotropy: polarization

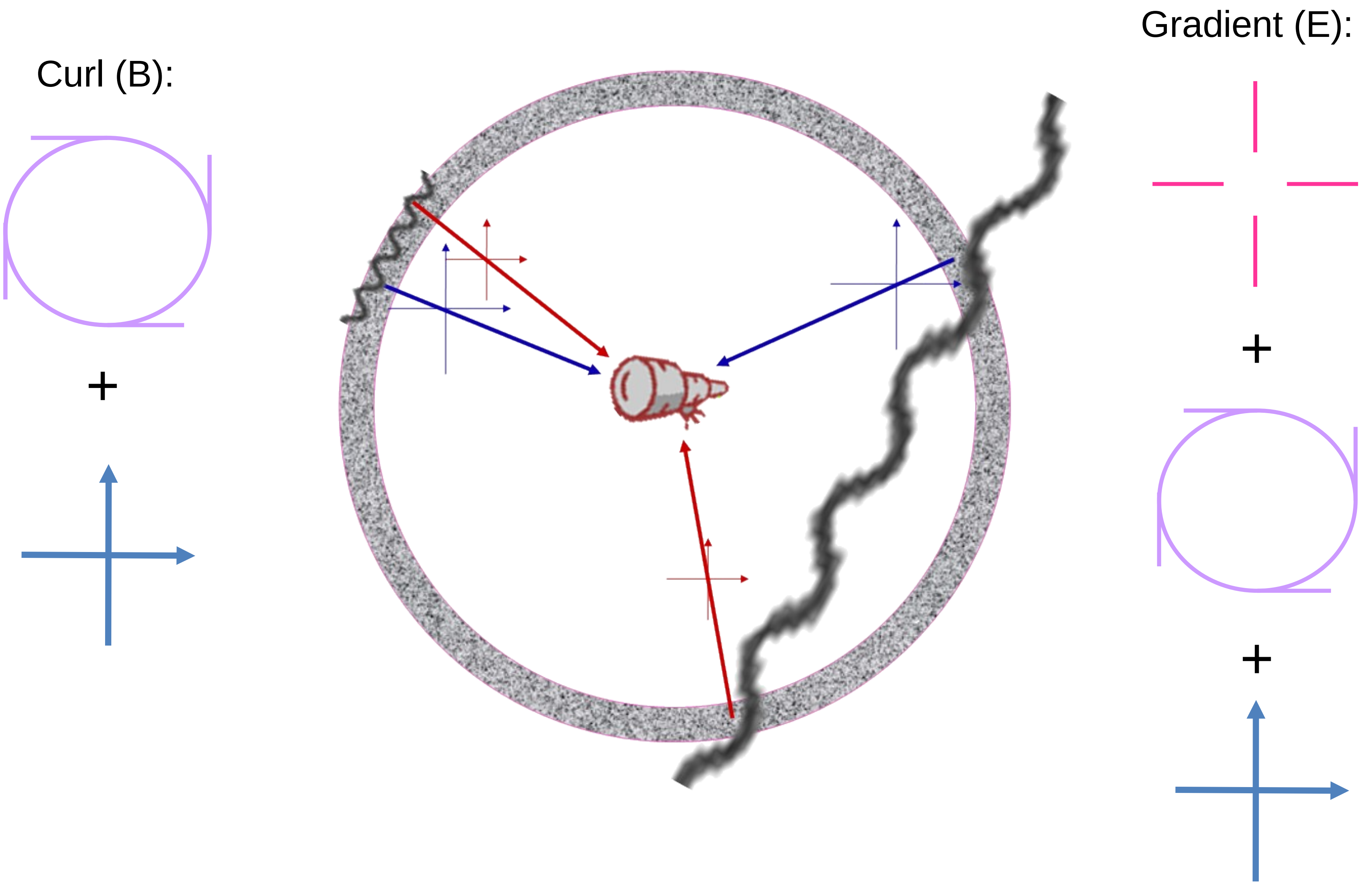

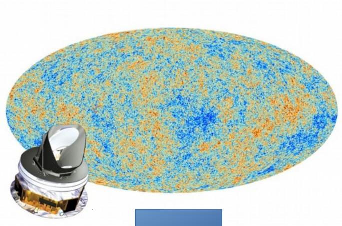

Anisotropies

$T(\theta,\varphi)$, $Q(\theta,\varphi)$, $U(\theta,\varphi)$, $V(\theta,\varphi)$

spherical harmonics

$X(\theta,\varphi)=\Sigma_{lm}\, a_{lm}^{X}\, Y^{s}_{lm}(\theta,\varphi)$

$X=T,E,B$

$s=0$ for T, 2 for Q and U

E and B modes have opposite parity

Angular power spectrum

$T(\theta,\varphi)$, $Q(\theta,\varphi)$, $U(\theta,\varphi)$, $V(\theta,\varphi)$

spherical harmonics

a^X_{lm}, $X=T,E,B$

information compression

$C_{l}=\Sigma_m [(a_{lm}^X)(a_{lm}^Y)^*]/(2l+1)$

CMB angular power spectrum

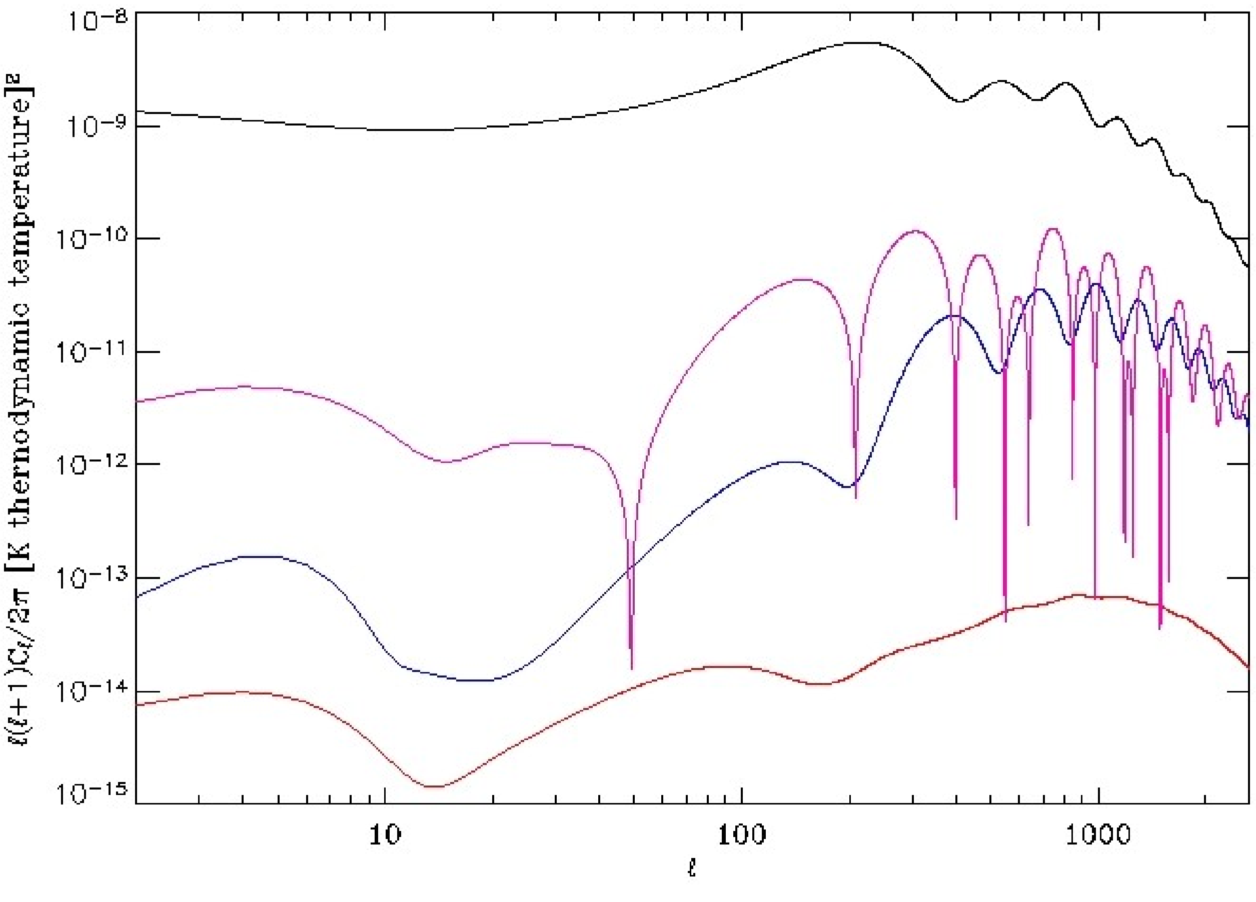

Angle ≈ 200/l degrees

CMB angular power spectrum

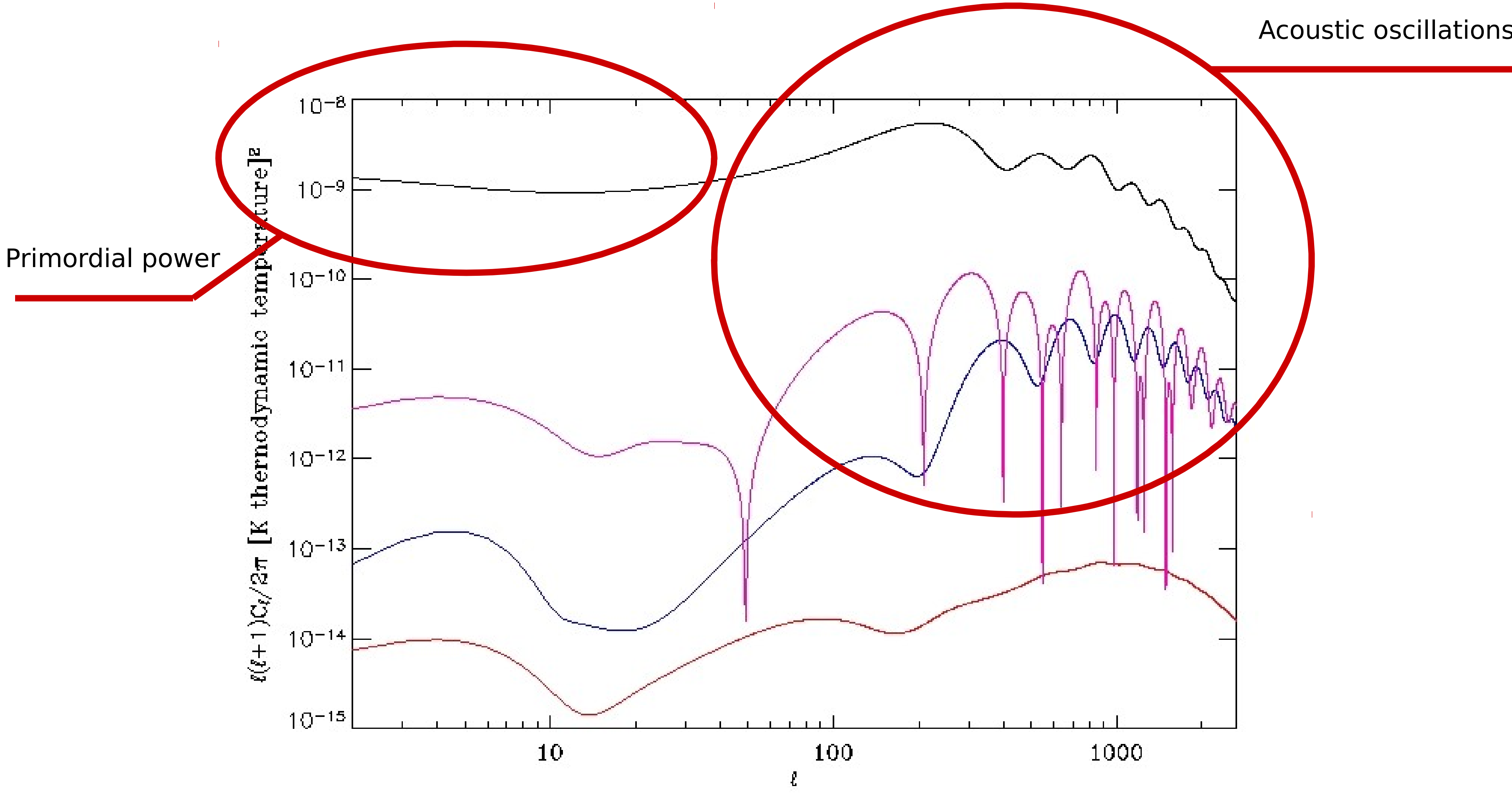

Angle ≈ 200/l degrees

CMB angular power spectrum

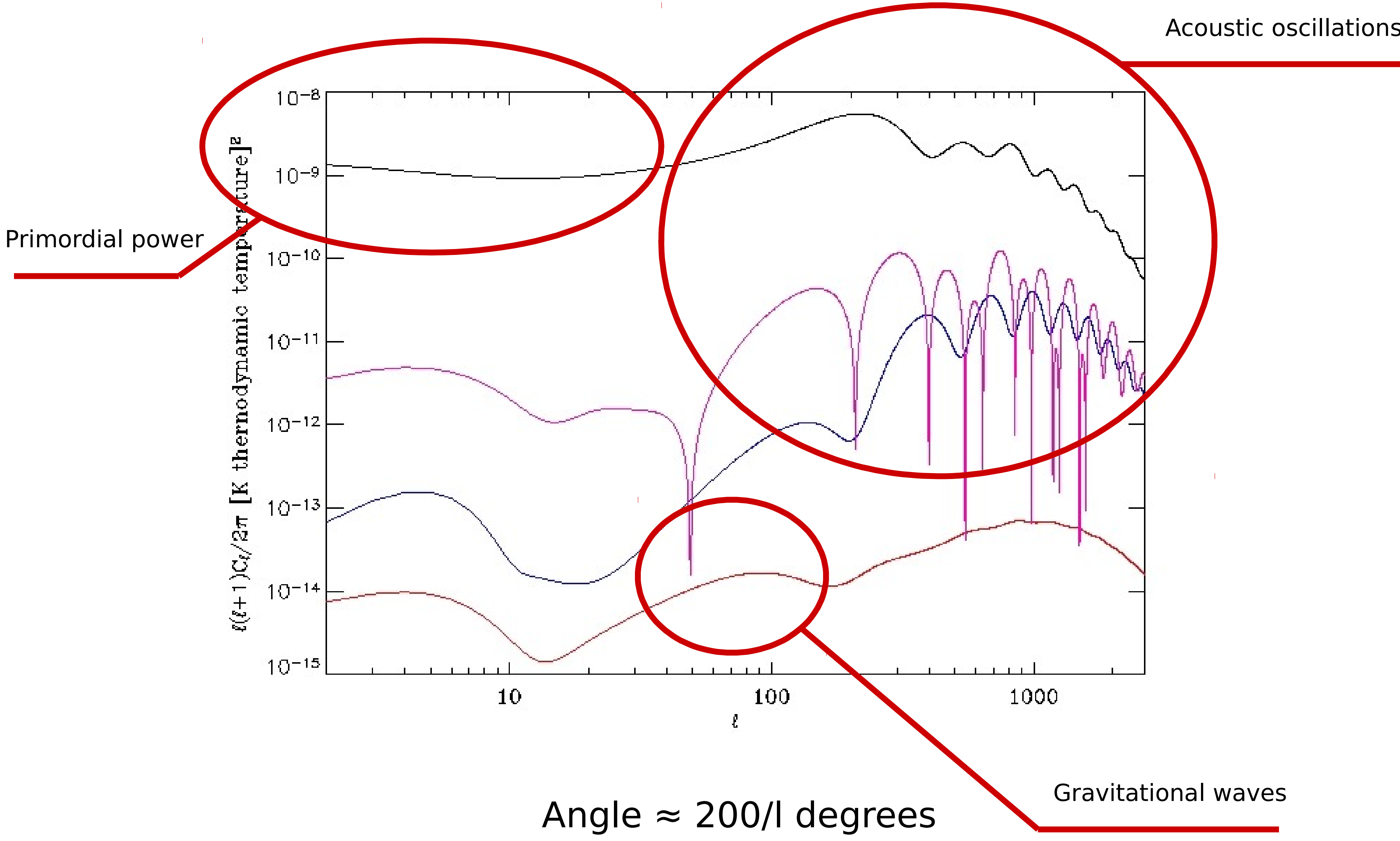

Angle ≈ 200/l degrees

The B-modes record GWs mono-chromatically in angle

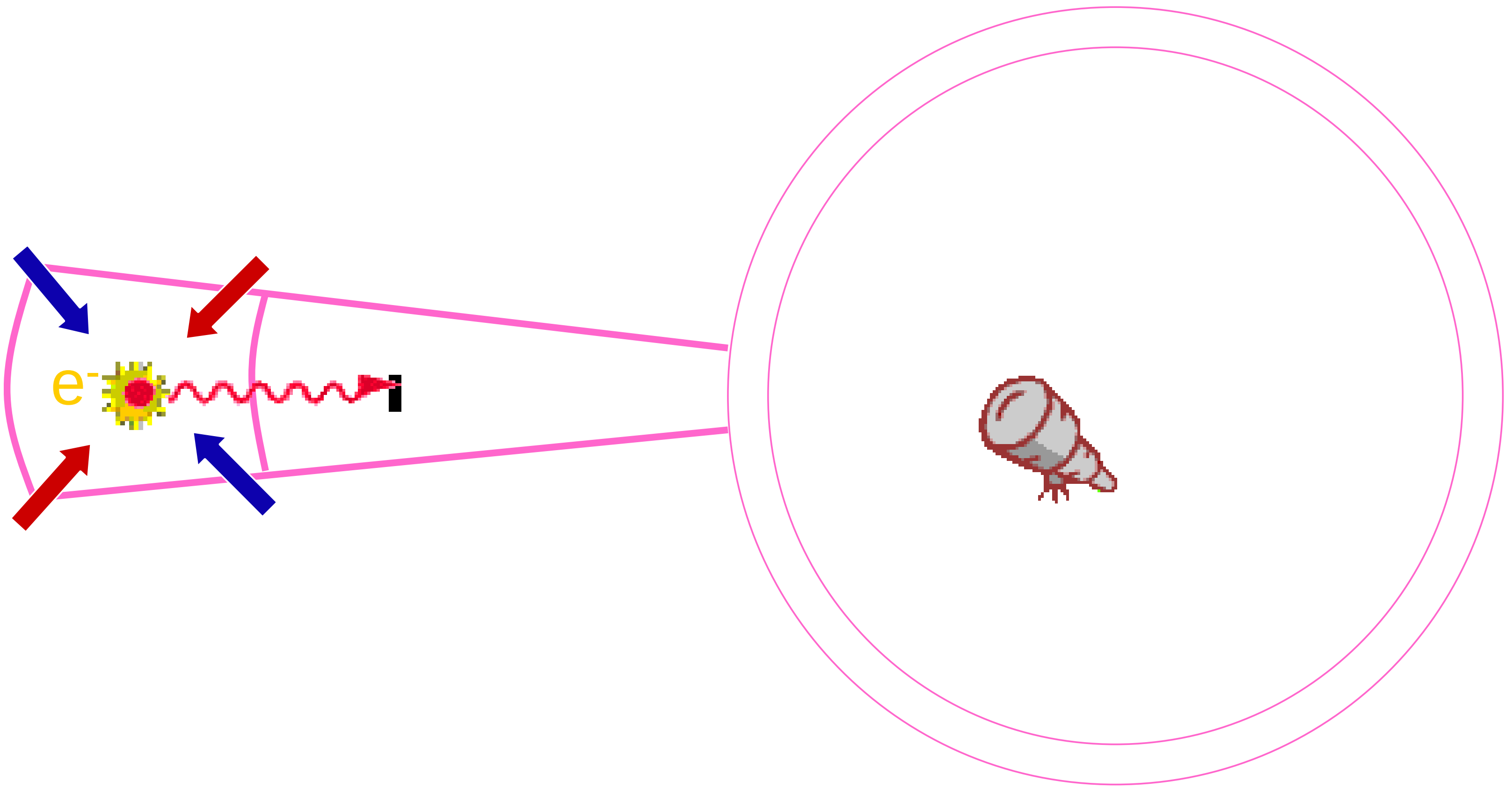

The B-modes record GWs mono-chromatically in angle

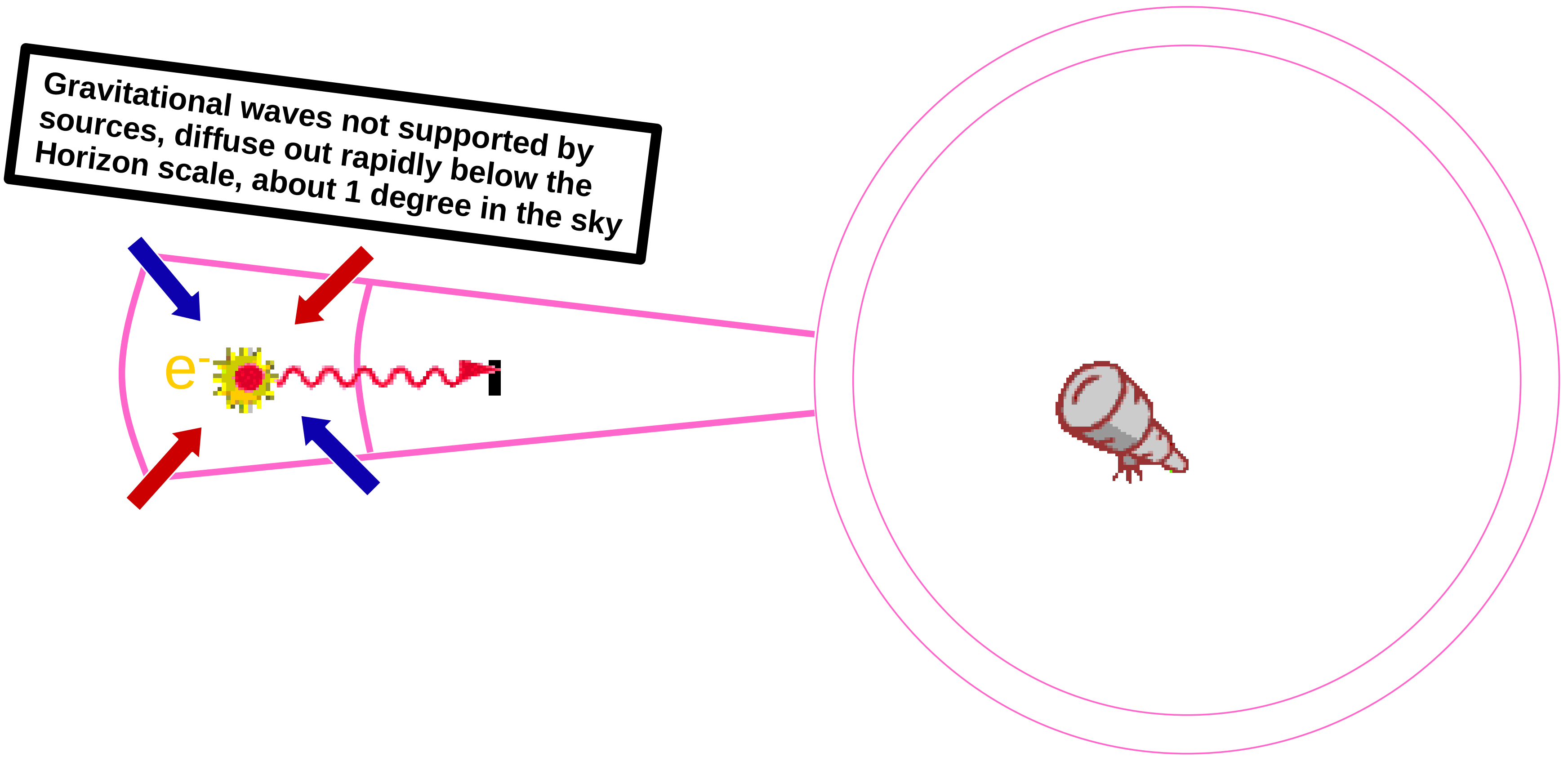

The B-modes record GWs mono-chromatically in angle

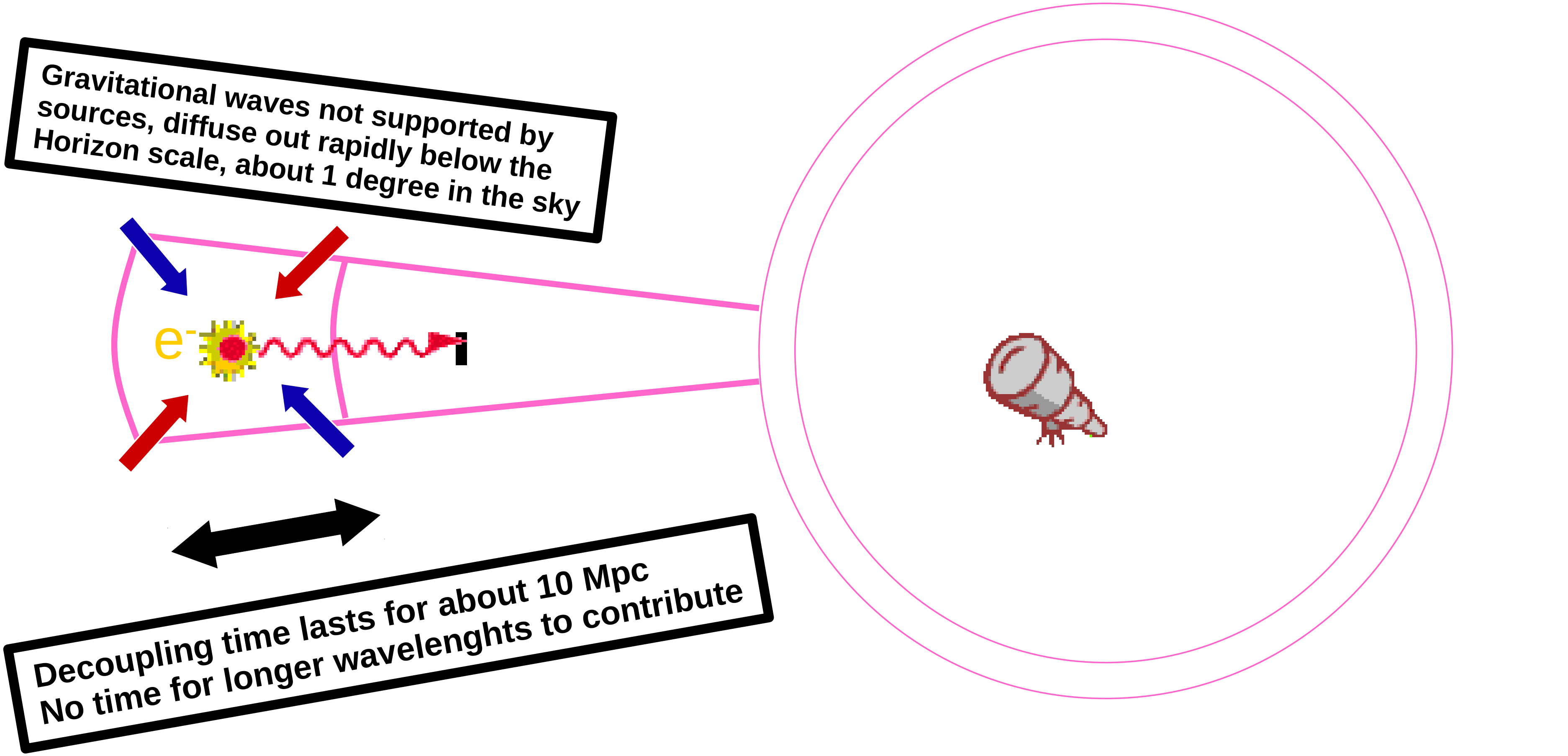

The B-modes record GWs mono-chromatically in angle

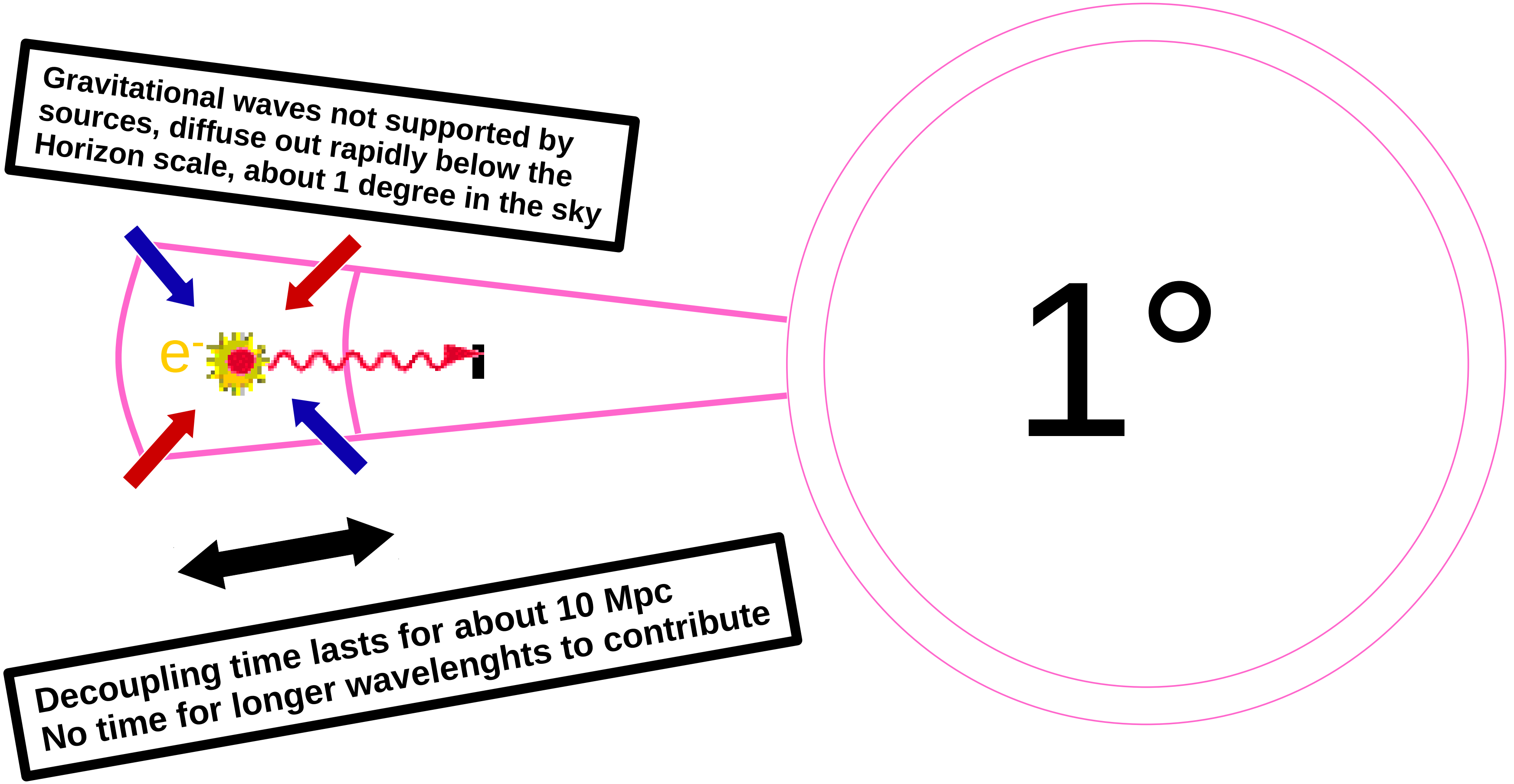

LSS effects on CMB

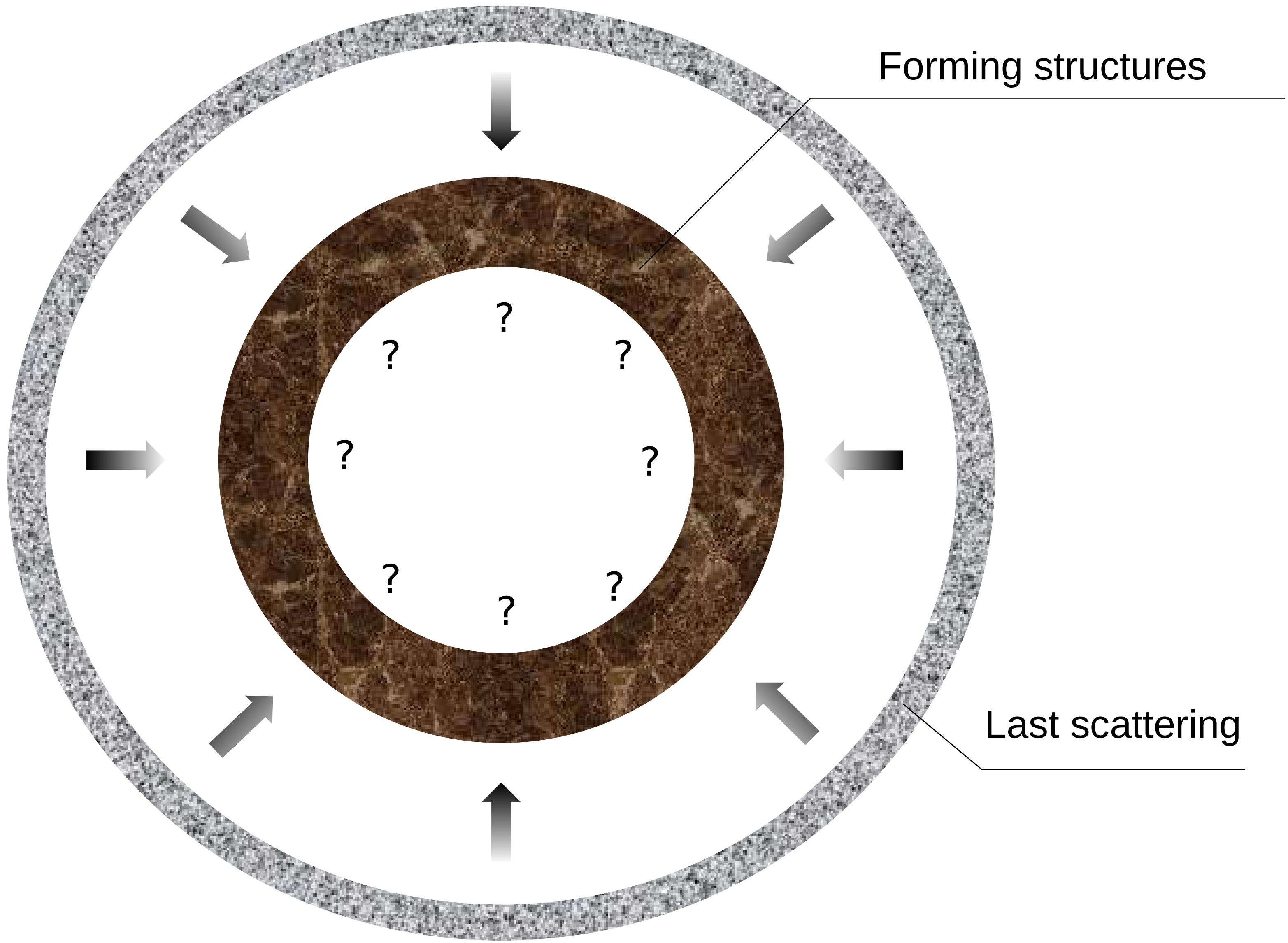

Categories for LSS effects on CMB

- Re-scattering
- Gravitation

Categories for LSS effects on CMB

- Re-scattering
  - Re-ionization
- Gravitation
  - Dynamics in the metric tensor
  - Deflection

Categories for LSS effects on CMB

- Re-scattering
  - Re-ionization
- Gravitation
  - Dynamics in the metric tensor
  - Deflection

CMB lensing

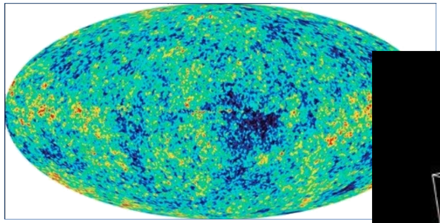

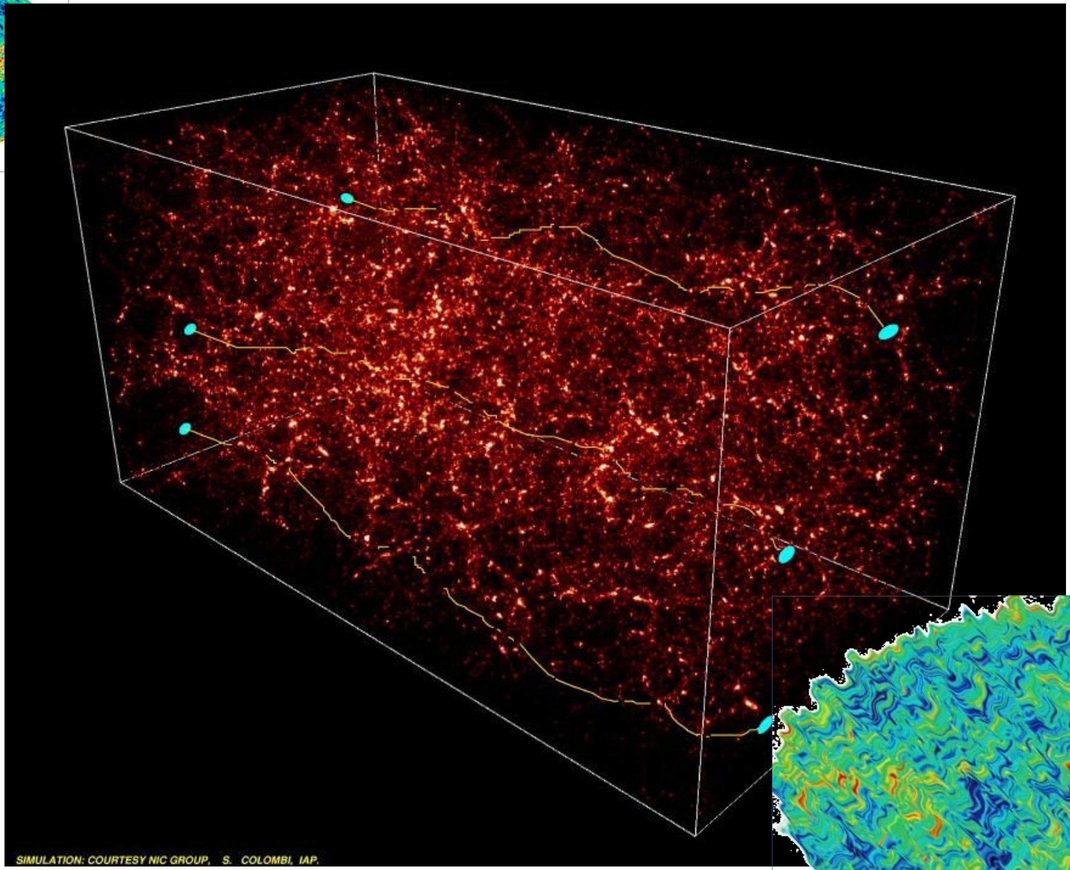

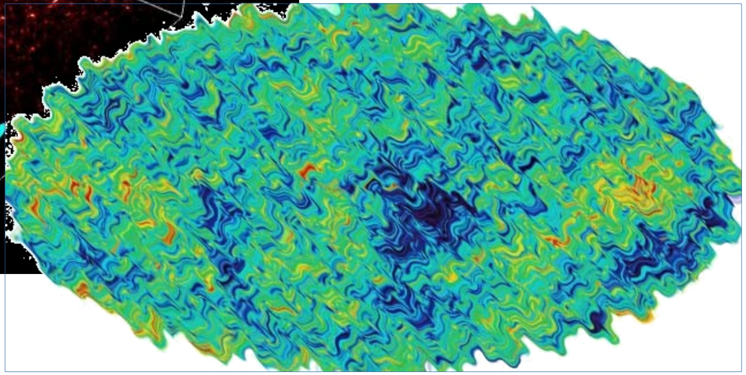

CMB lensing

T

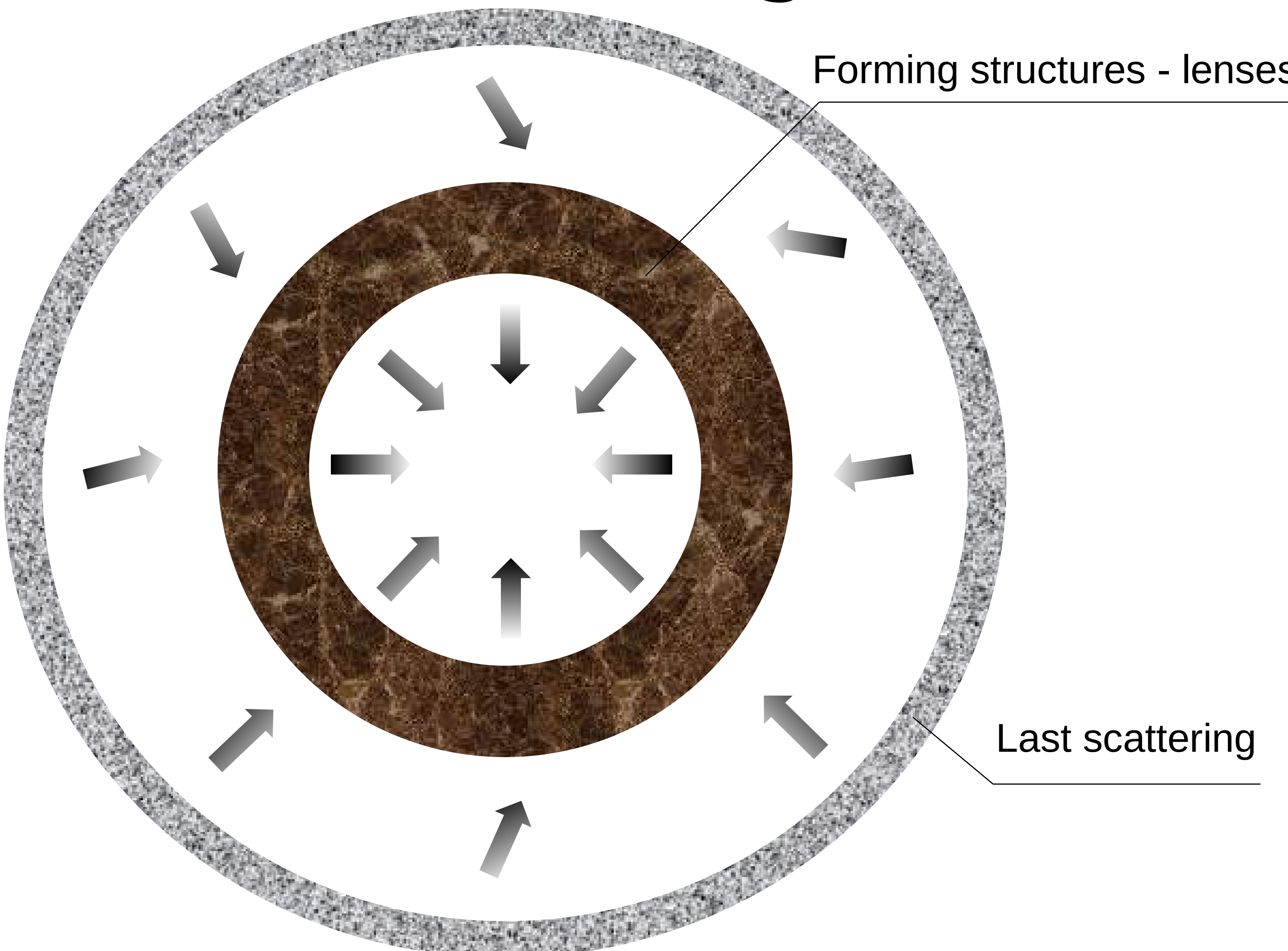

Bartelmann, Schneider 2001, Hu 2000

CMB lensing

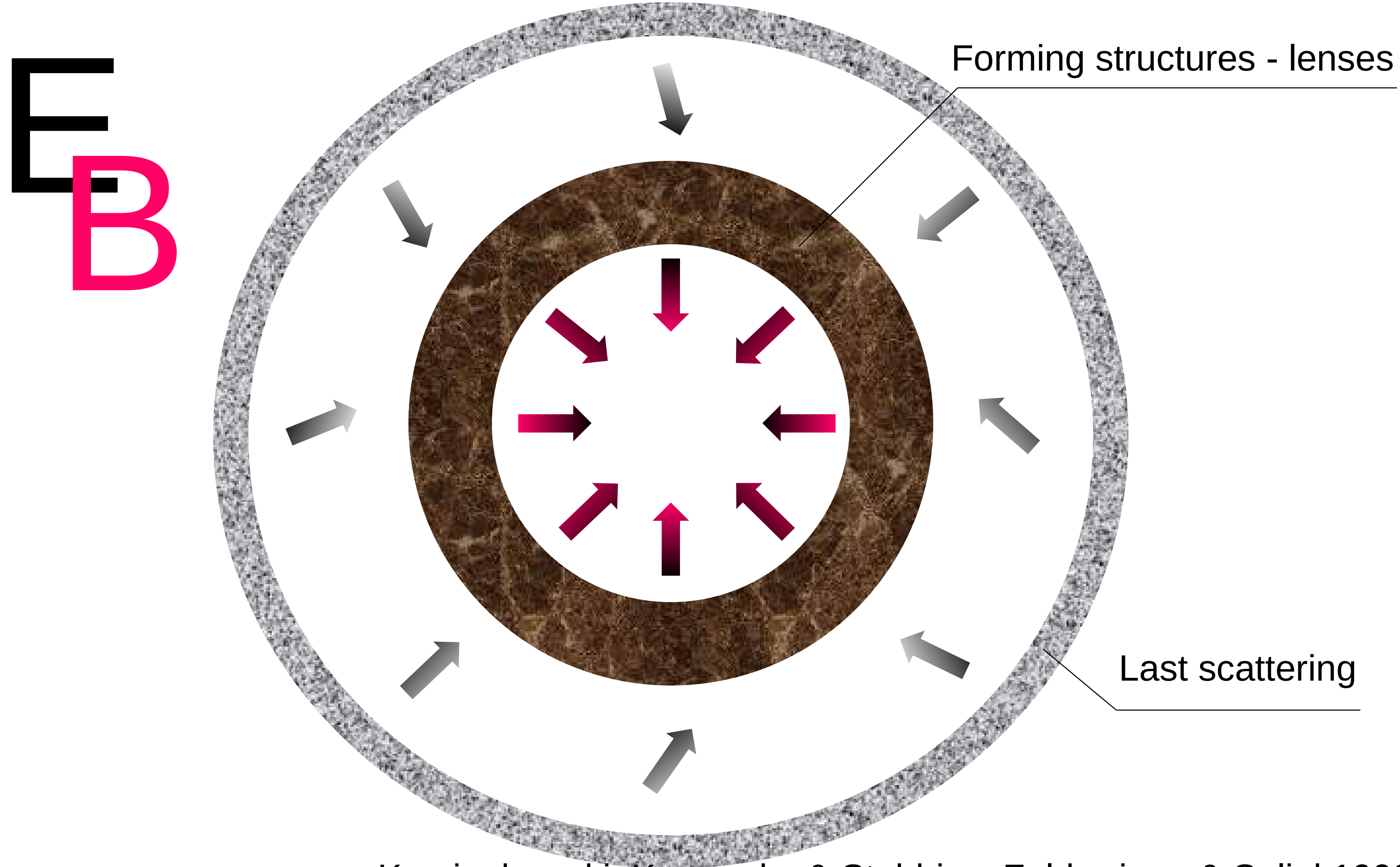

Kamionkowski, Kosowsky & Stebbins, Zaldarriaga & Seljak1998

CMB lensing

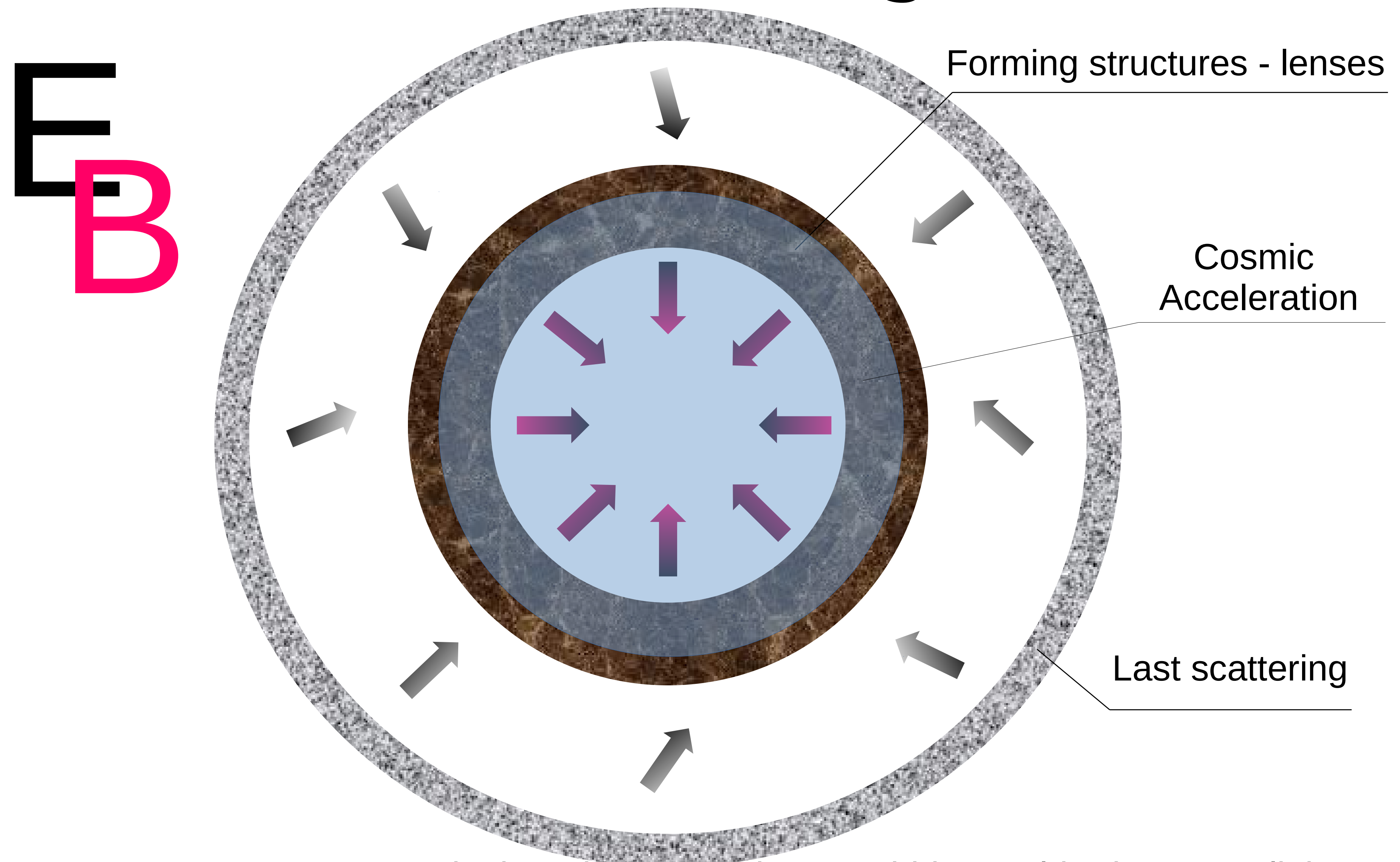

Kamionkowski, Kosowsky & Stebbins, Zaldarriaga & Seljak1998

CMB angular power spectrum

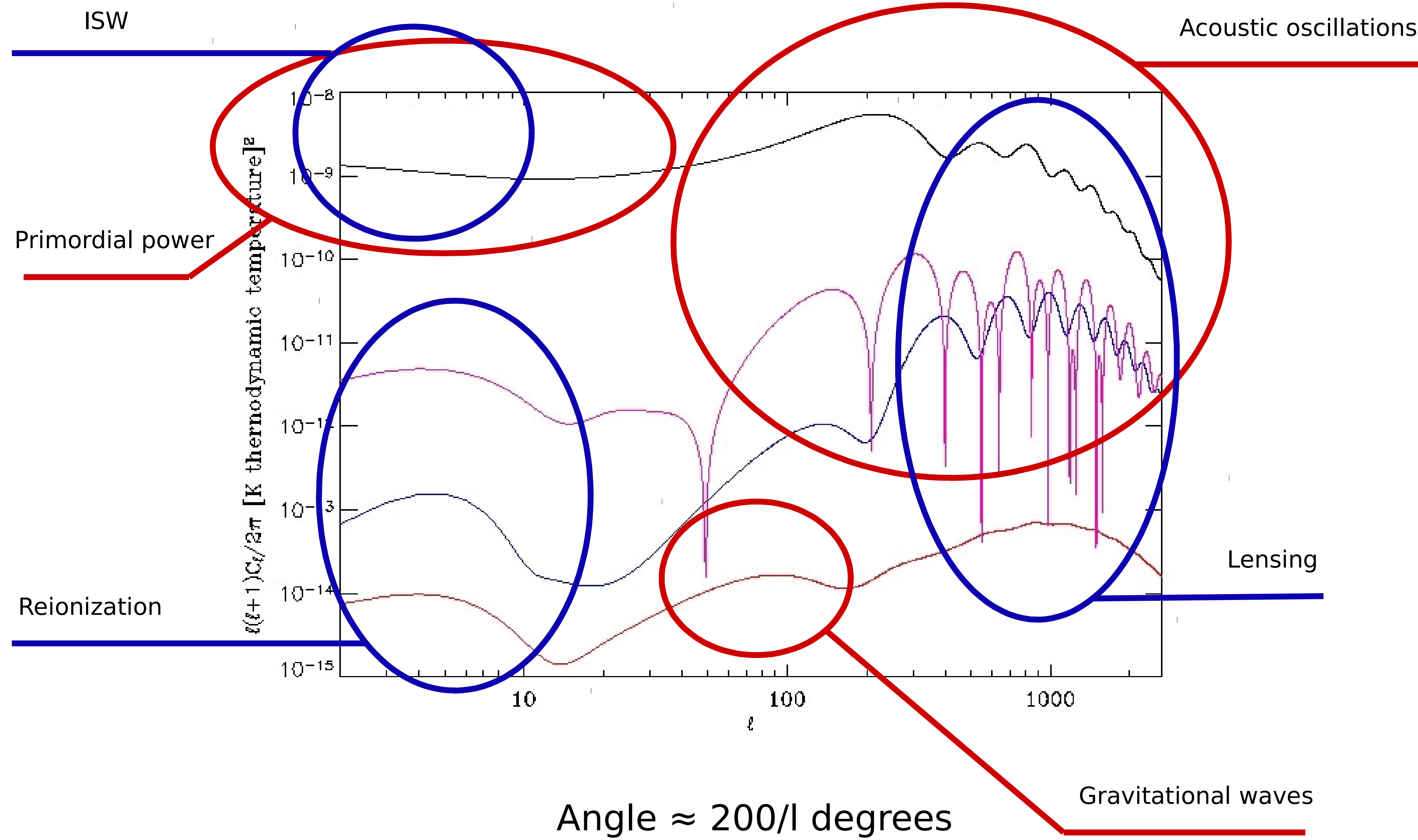

Angle ≈ 200/l degrees

Dark Energy Effects on CMB

- Modified background evolution
  - Projection: distance to recombination is modified, causing a projection of features in the CMB
  - Late Integrated Sachs-Wolfe: gravitational potentials evolve differently from a pure ΛCDM
  - Lensing: potential evolve differently from a pure ΛCDM
- Modified perturbation behavior
  - Large Scale Clustering
  - Modified Gravity: Generalized Poisson and Stress-Energy equations

Expansion and Clustering

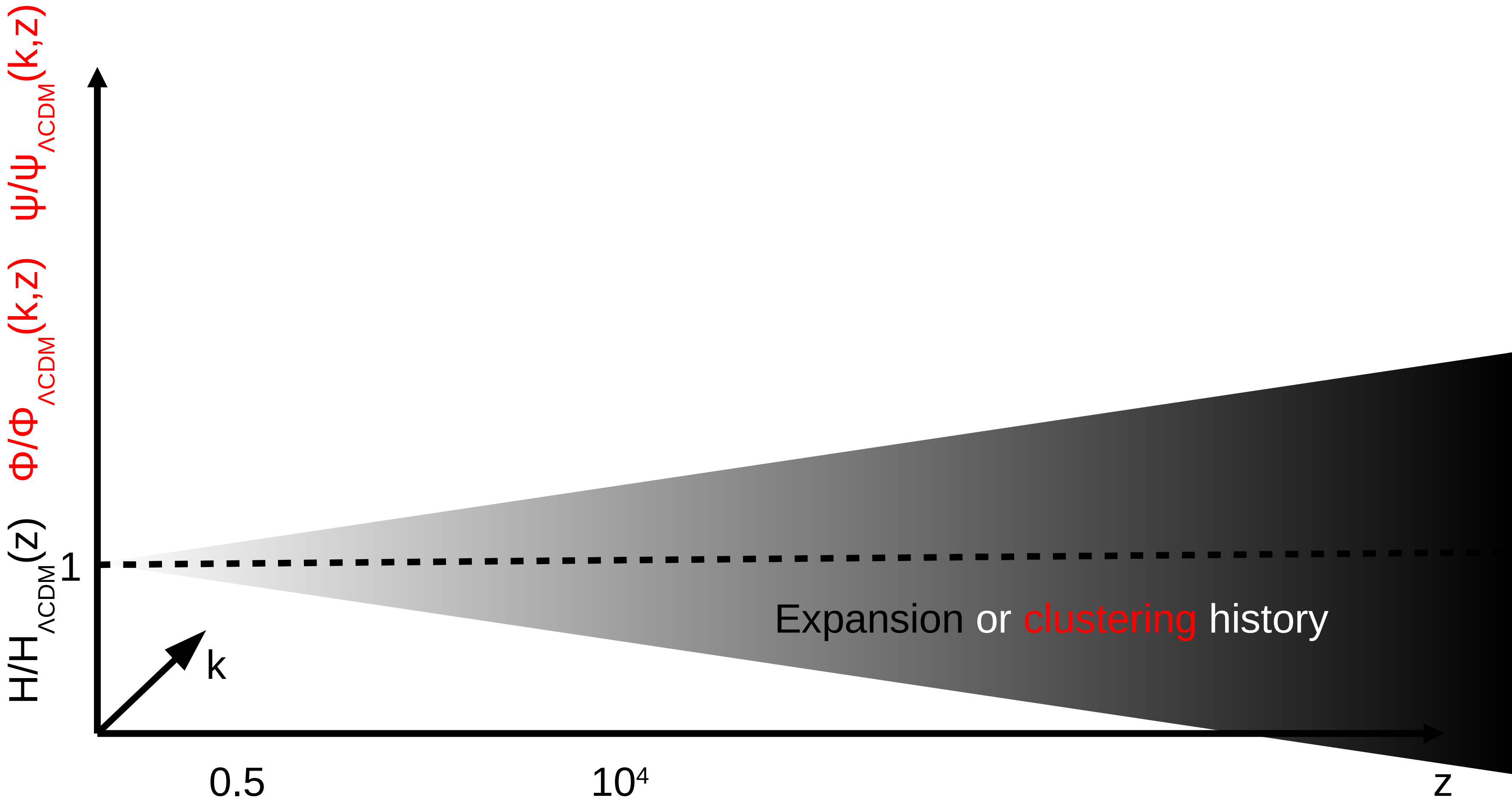

Expansion and Clustering

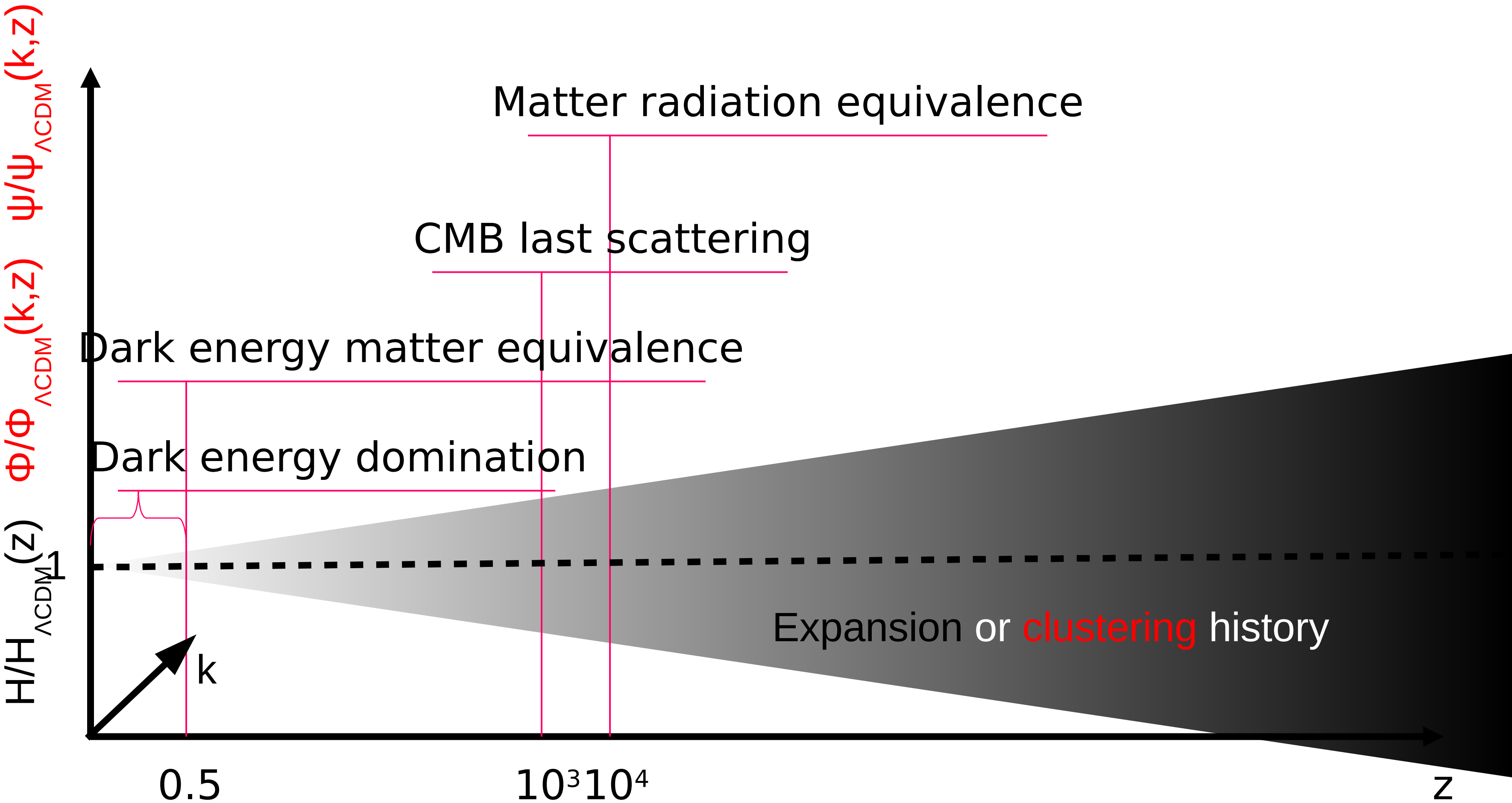

Expansion and Clustering

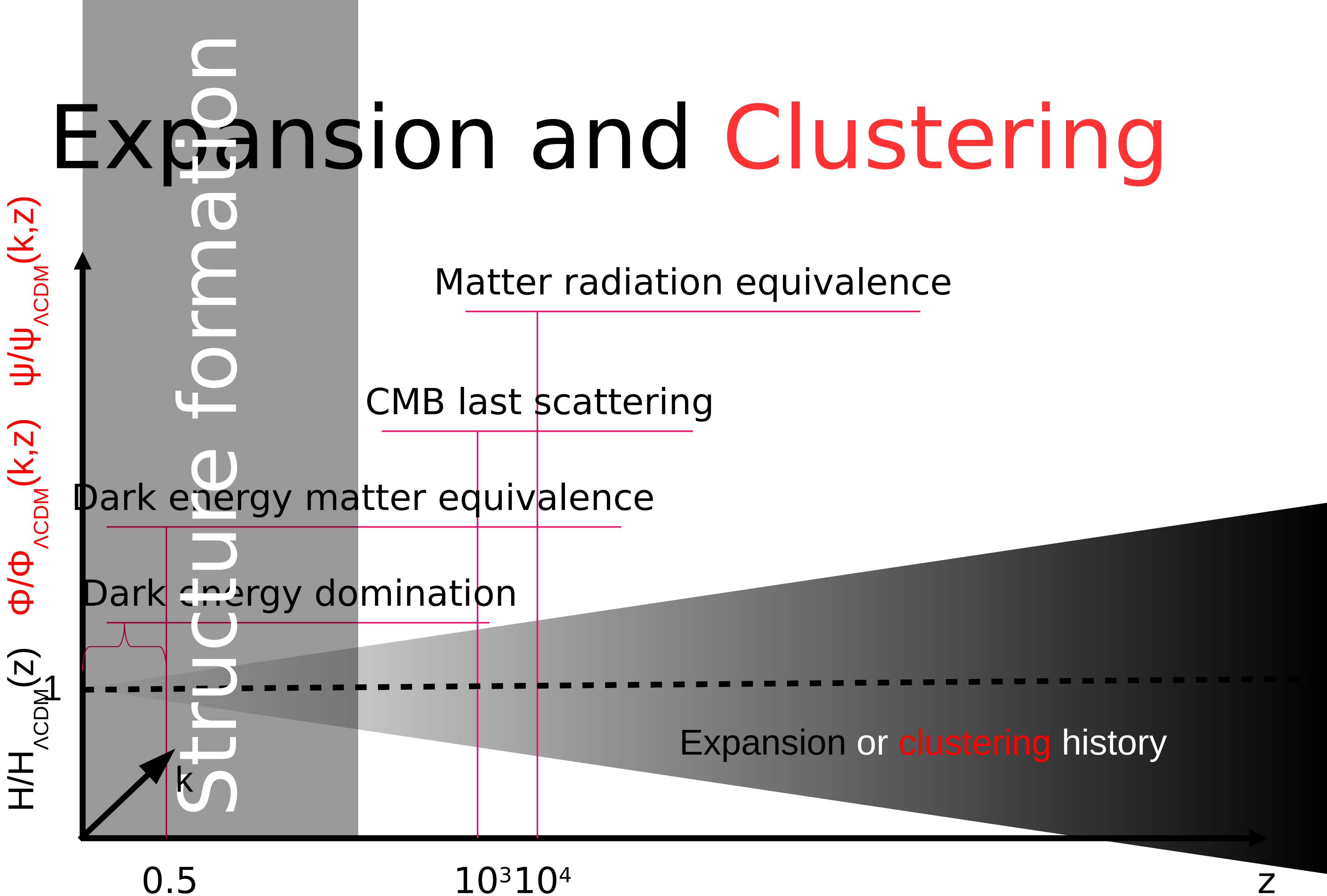

Expansion and clustering histories

$$D = H_0^{-1}\int_0^z \frac{dz}{\left[\sum_i \Omega_i (1+z)^{3(1+w_i)}\right]^{1/2}}$$

$$k^2(\Phi+\Psi) = -8\pi G a^2 \rho \Pi$$

$$k^2\Phi = 4\pi G a^2 \rho \delta$$

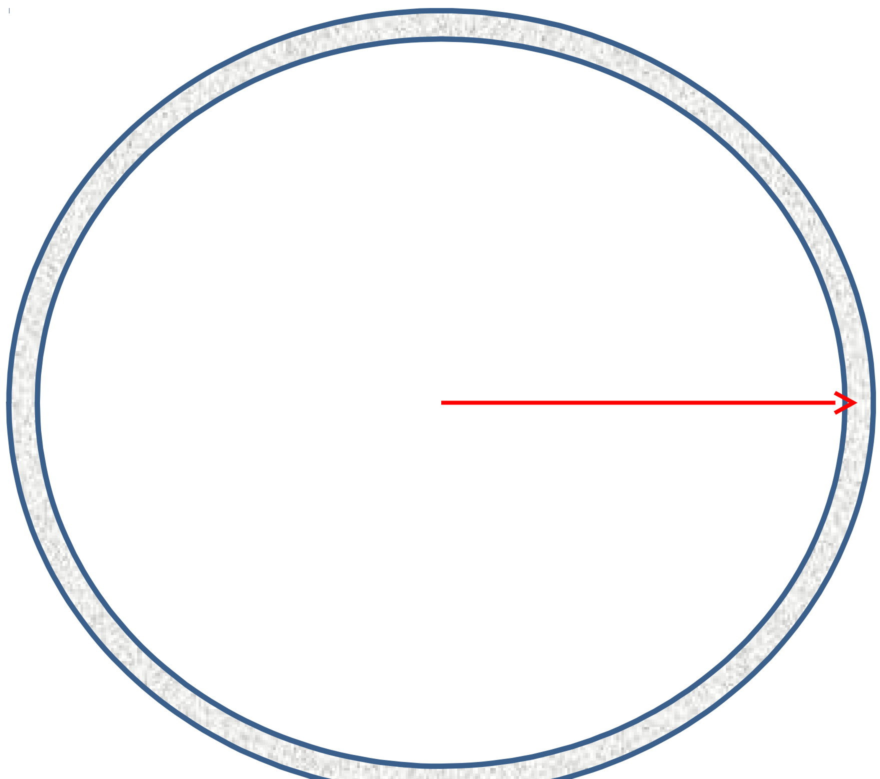

Expansion and clustering histories

$$D = H_0^{-1}\int_0^z \frac{dz}{\left[\Sigma_i \Omega_i (1+z)^{3(1+w_i)}\right]^{1/2}}$$

$$k^2(\Phi+\Psi) = -8\pi G a^2 \rho \Pi$$

$$k^2\Phi = 4\pi G a^2 \rho \delta$$

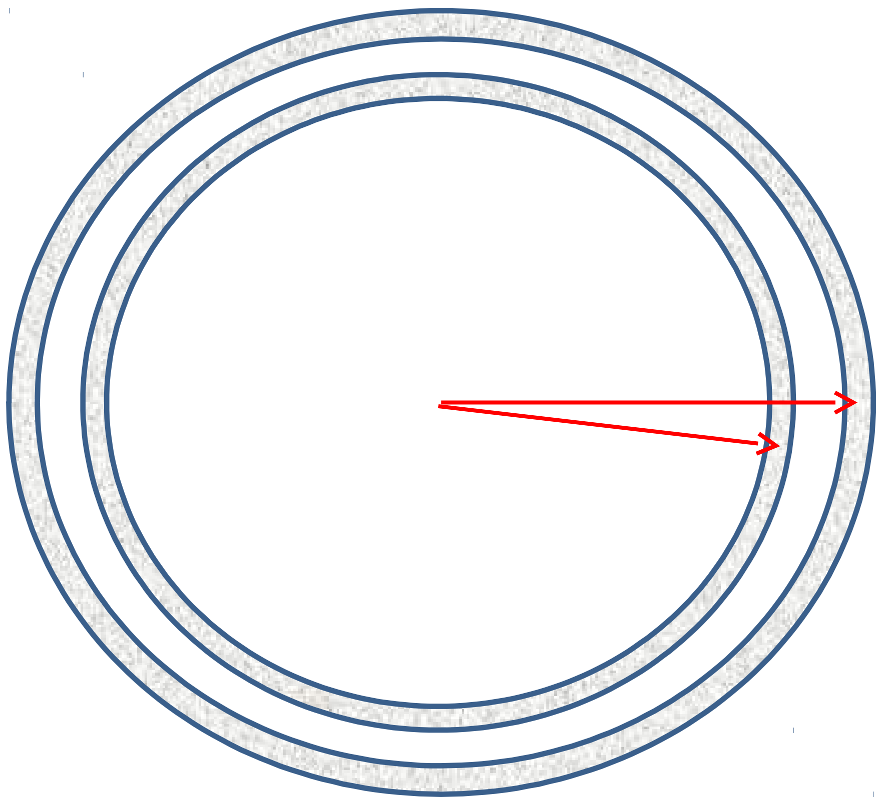

Expansion and clustering histories

$$D = H_0^{-1} \int_0^z \frac{dz}{\left[\sum_i \Omega_i (1+z)^{3(1+w_i)}\right]^{1/2}}$$

$$k^2(\Phi+\Psi) = -8\pi G a^2 \rho \Pi$$

$$k^2 \Phi = 4\pi G a^2 \rho \delta$$

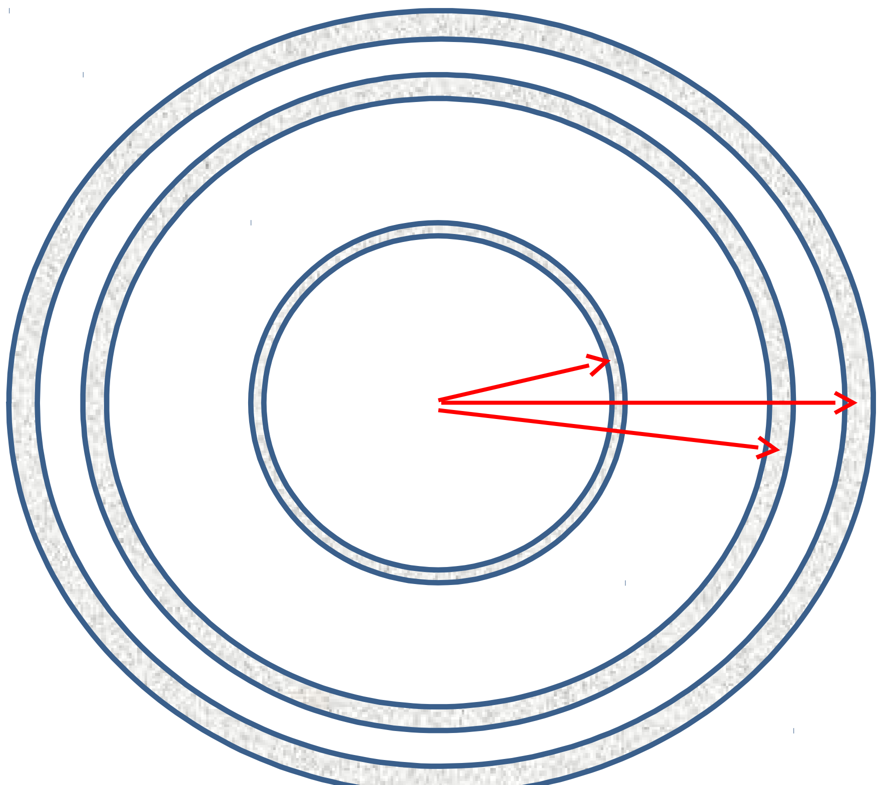

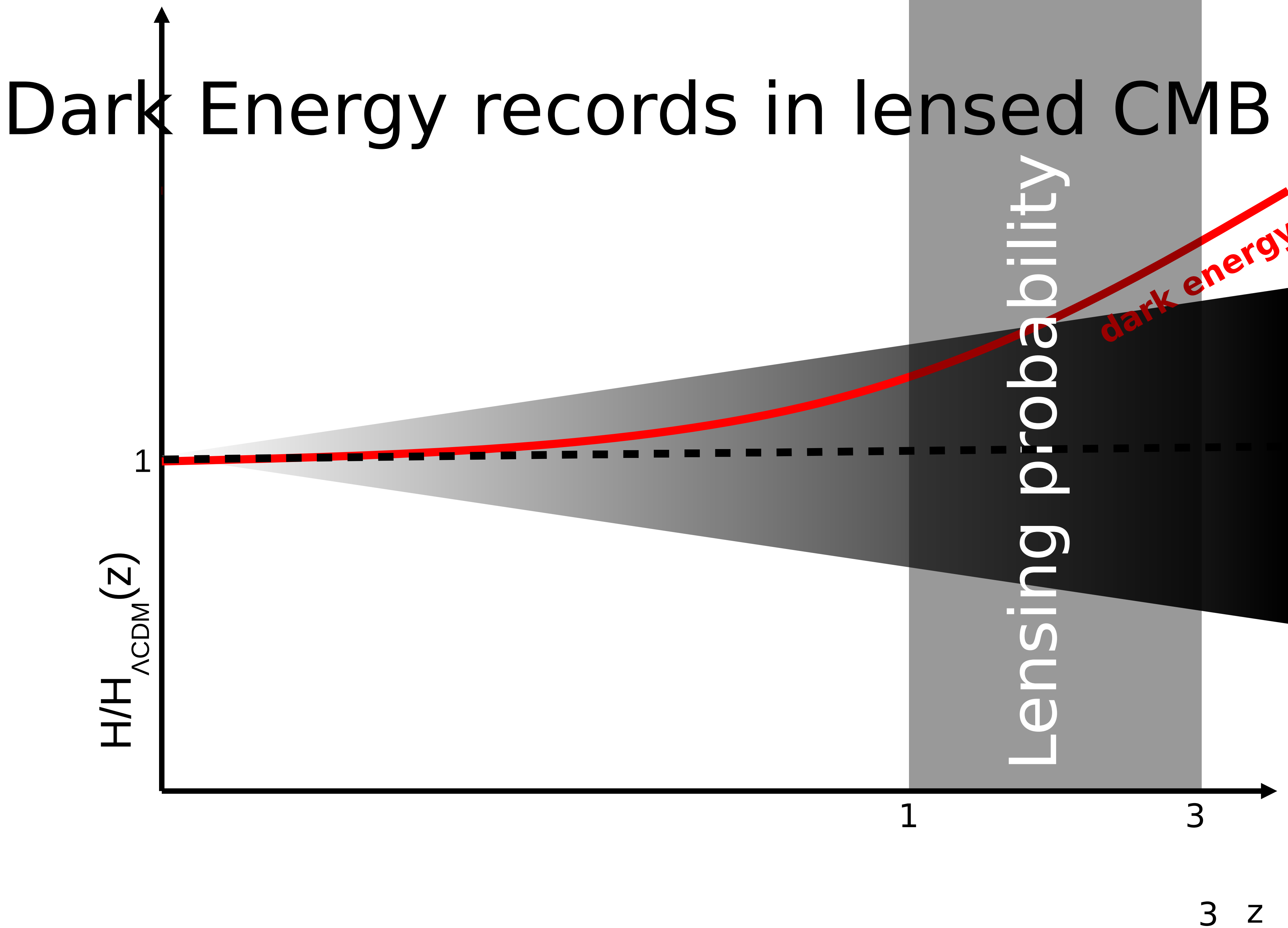

Dark Energy records in lensed CMB
Lensing probability
dark energy
$H/H_{\Lambda CDM}(z)$
1
1
3
3
z

Dark Energy Parametrizations

- Background
  - First order expansion of w(z) at low redshifts
  - Principal components of w(z)
  - Direct predictions from models
- Perturbations
  - New functions describing departures from General Relativity equations
  - Effective Field Theory
  - Direct predictions from models

Background: First Order Expansion

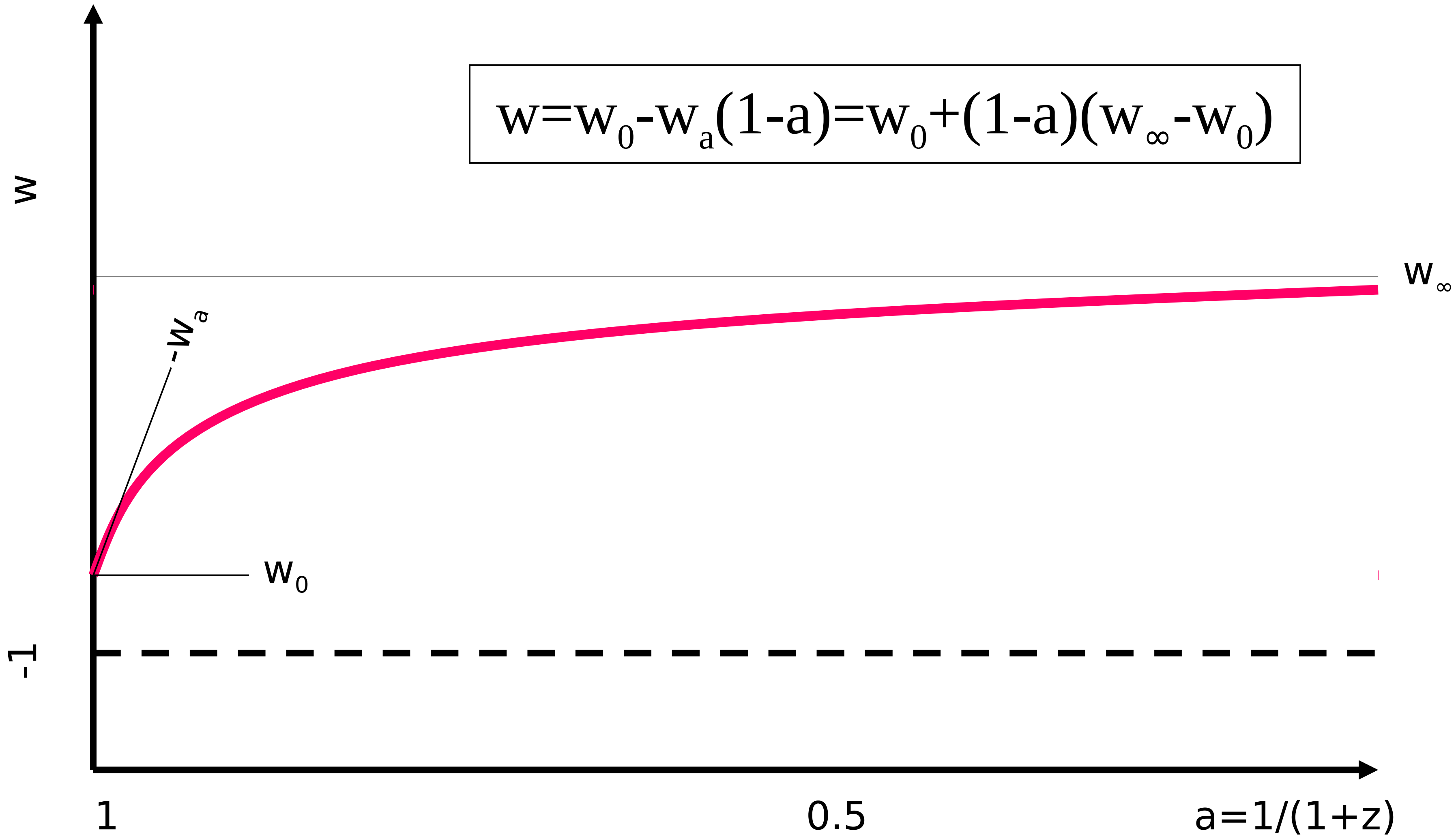

Chevallier & Polarski 2001, Linder 2003

Background: Principal Components

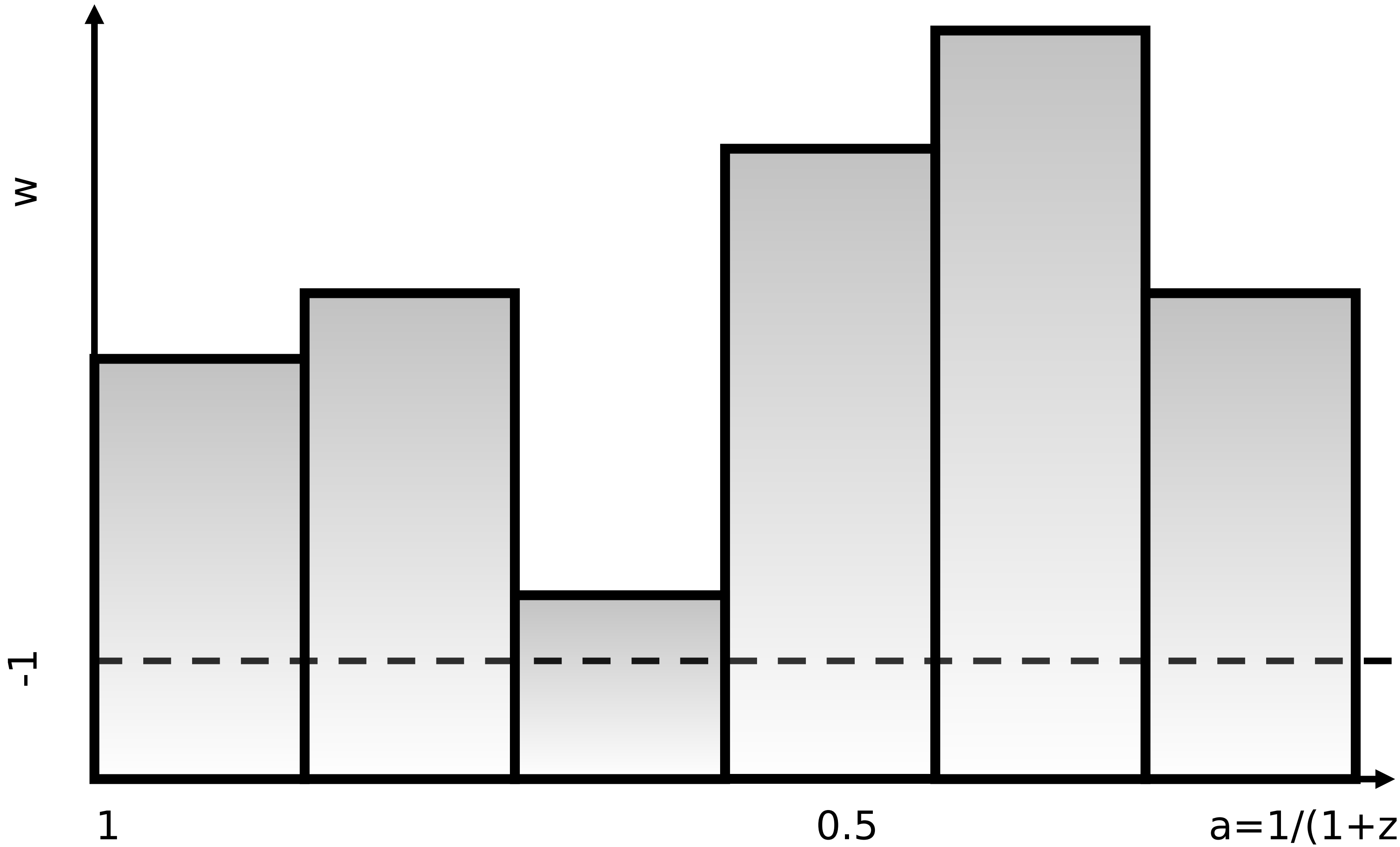

Crittenden & Pogosian 2006, Dick et al. 2006,Said et al. 2013

Perturbations

Effective Field Theory:

$$S = \int d^4x \sqrt{-g} \left\{ \frac{m_0^2}{2} [1 + \Omega(\tau)] R + \Lambda(\tau) - a^2 c(\tau) \delta g^{00} + \frac{M_2^4(\tau)}{2} \left(a^2 \delta g^{00}\right)^2 - \bar{M}_1^3(\tau) 2a^2 \delta g^{00} \delta K_\mu^\mu - \frac{\bar{M}_2^2(\tau)}{2} \left(\delta K_\mu^\mu\right)^2 - \frac{\bar{M}_3^2(\tau)}{2} \delta K_\nu^\mu \delta K_\mu^\nu + \frac{a^2 \hat{M}^2(\tau)}{2} \delta g^{00} \delta R^{(3)} + m_2^2(\tau) (g^{\mu\nu} + n^\mu n^\nu) \partial_\mu \left(a^2 g^{00}\right) \partial_\nu \left(a^2 g^{00}\right) \right\} + S_m[\chi_i, g_{\mu\nu}].$$

Modified Gravity:

$\eta(a, k) \equiv \Phi/\Psi.$

$-k^2 \Phi \equiv 4\pi G a^2 Q(a, k) \rho\Delta$

$-k^2 \Psi \equiv 4\pi G a^2 \eta(a, k) \rho\Delta$

$-k^2 (\Phi + \Psi) \equiv 8\pi G a^2 \Sigma(a, k) \rho\Pi$

Status of observations and challenges

Planck 2018

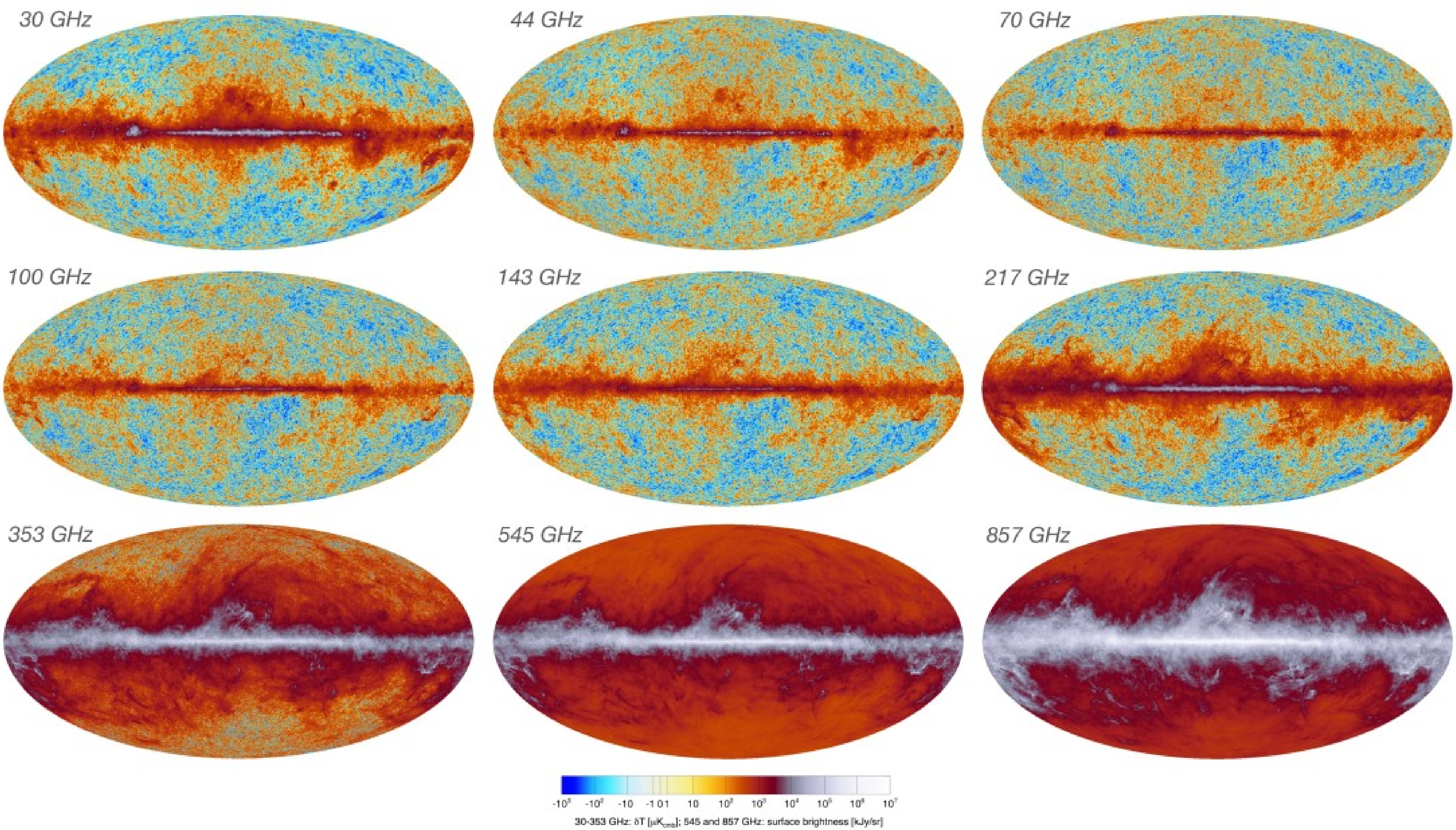
30 GHz
44 GHz
70 GHz
100 GHz
143 GHz
217 GHz
353 GHz
545 GHz
857 GHz
-10^3 -10^2 -10 -1 0 1 10 10^2 10^3 10^4 10^5 10^6 10^7
30-353 GHz: δT [μK_{cmb}]; 545 and 857 GHz: surface brightness [kJy/sr]

Planck 2018

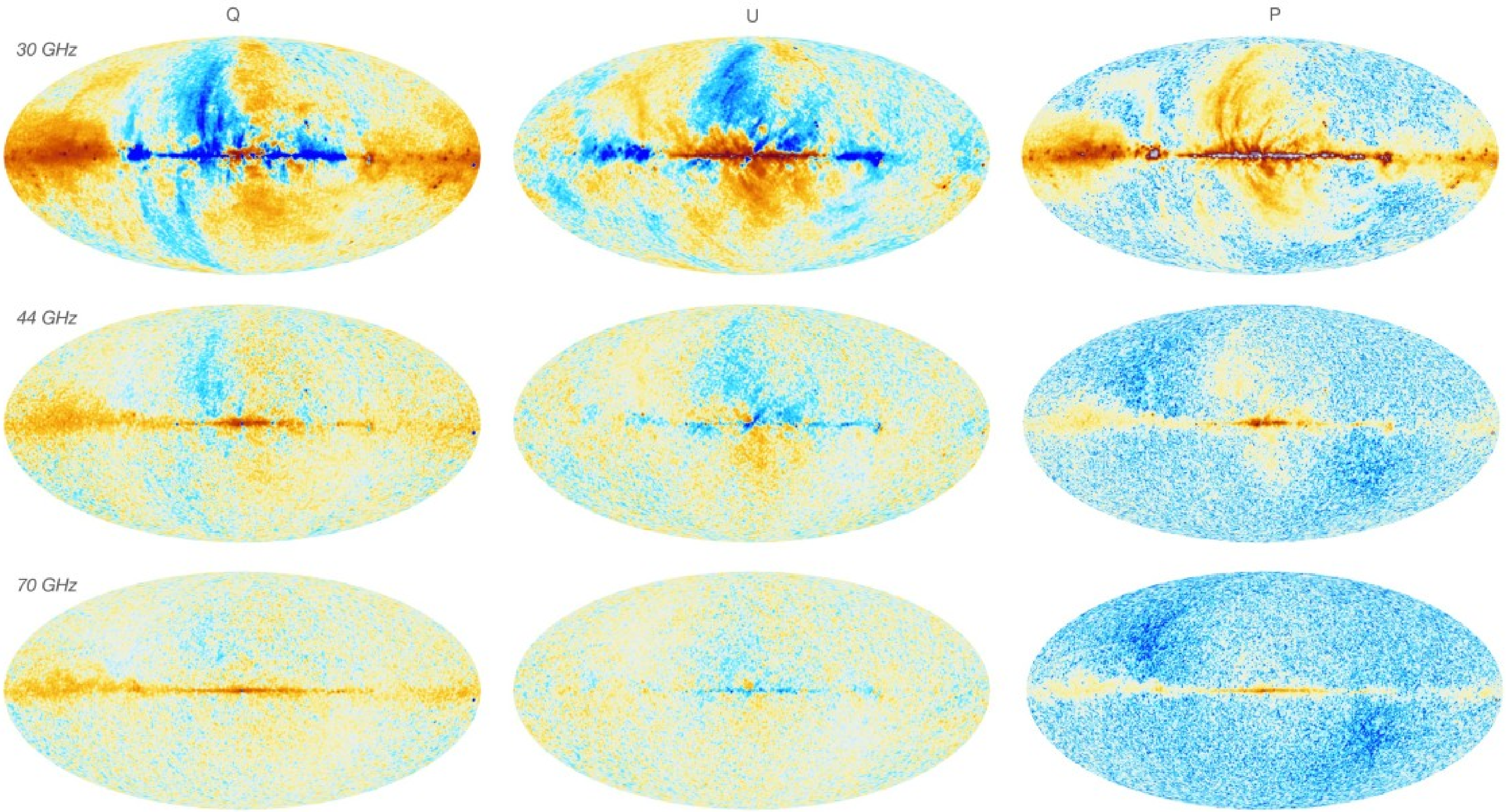

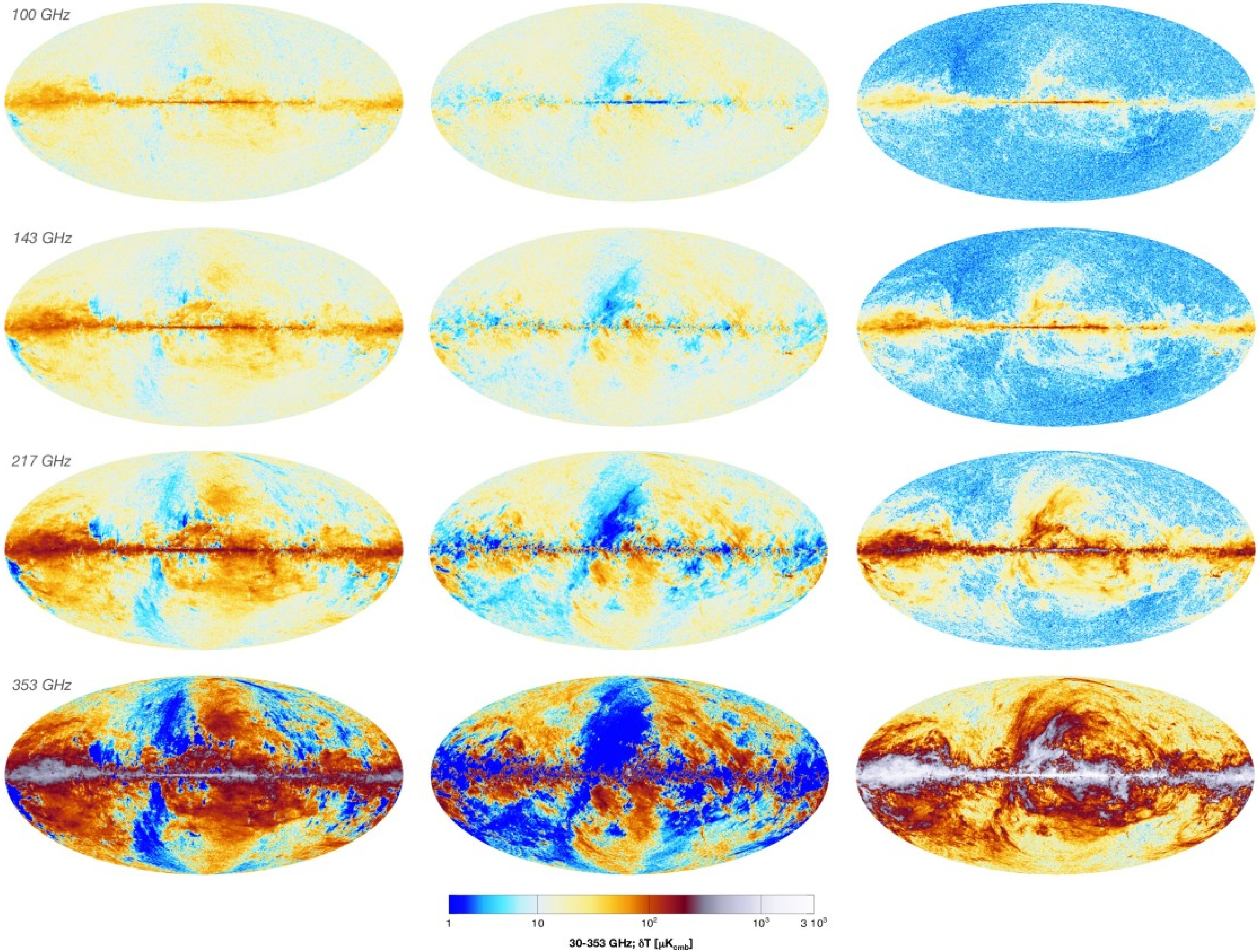
100 GHz
143 GHz
217 GHz
353 GHz
1
10
10^2
10^3
3 10^3
30-353 GHz; δT [μK_cmb]

Planck 2018

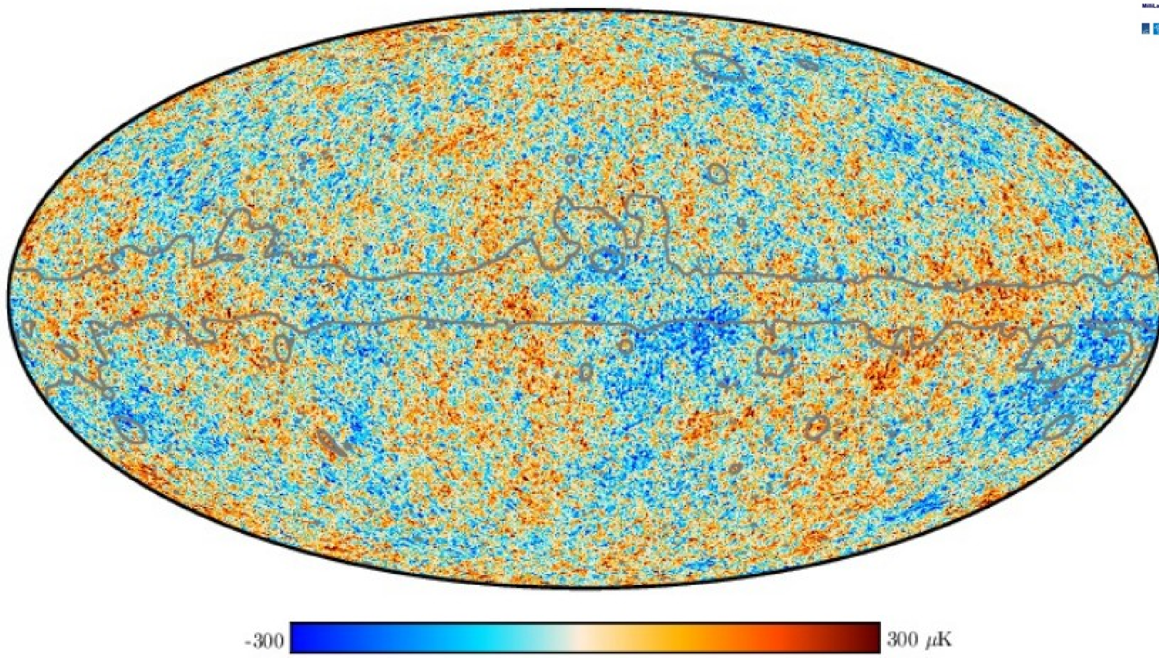

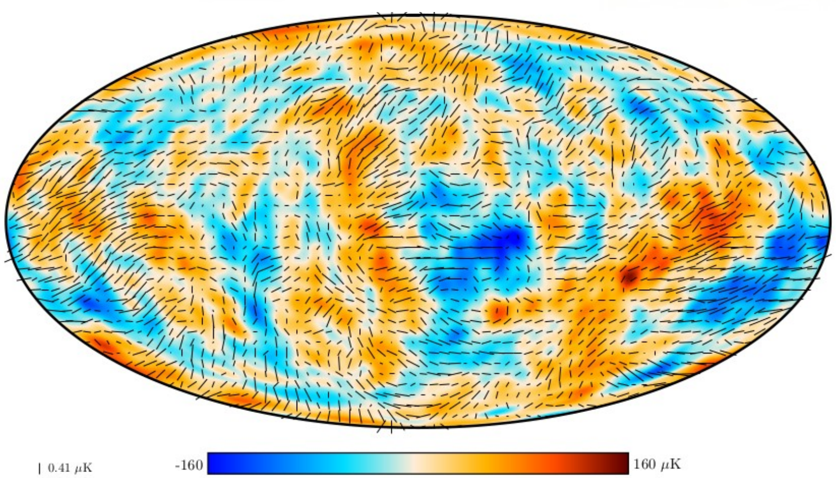

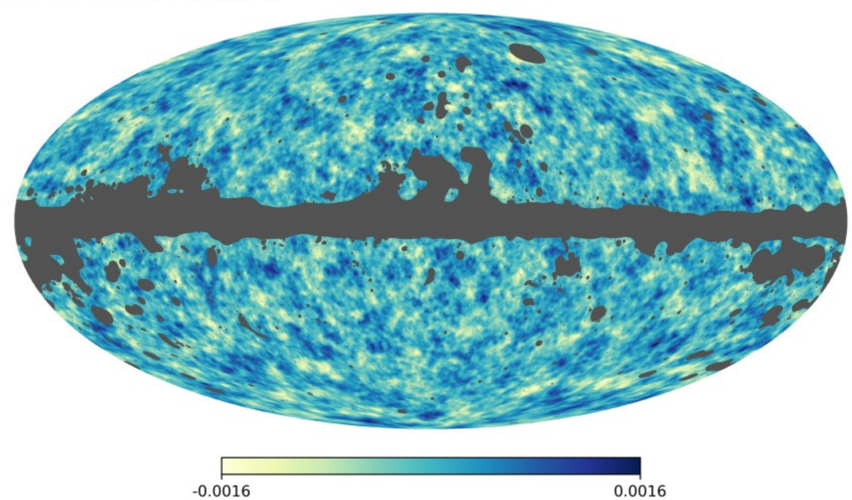

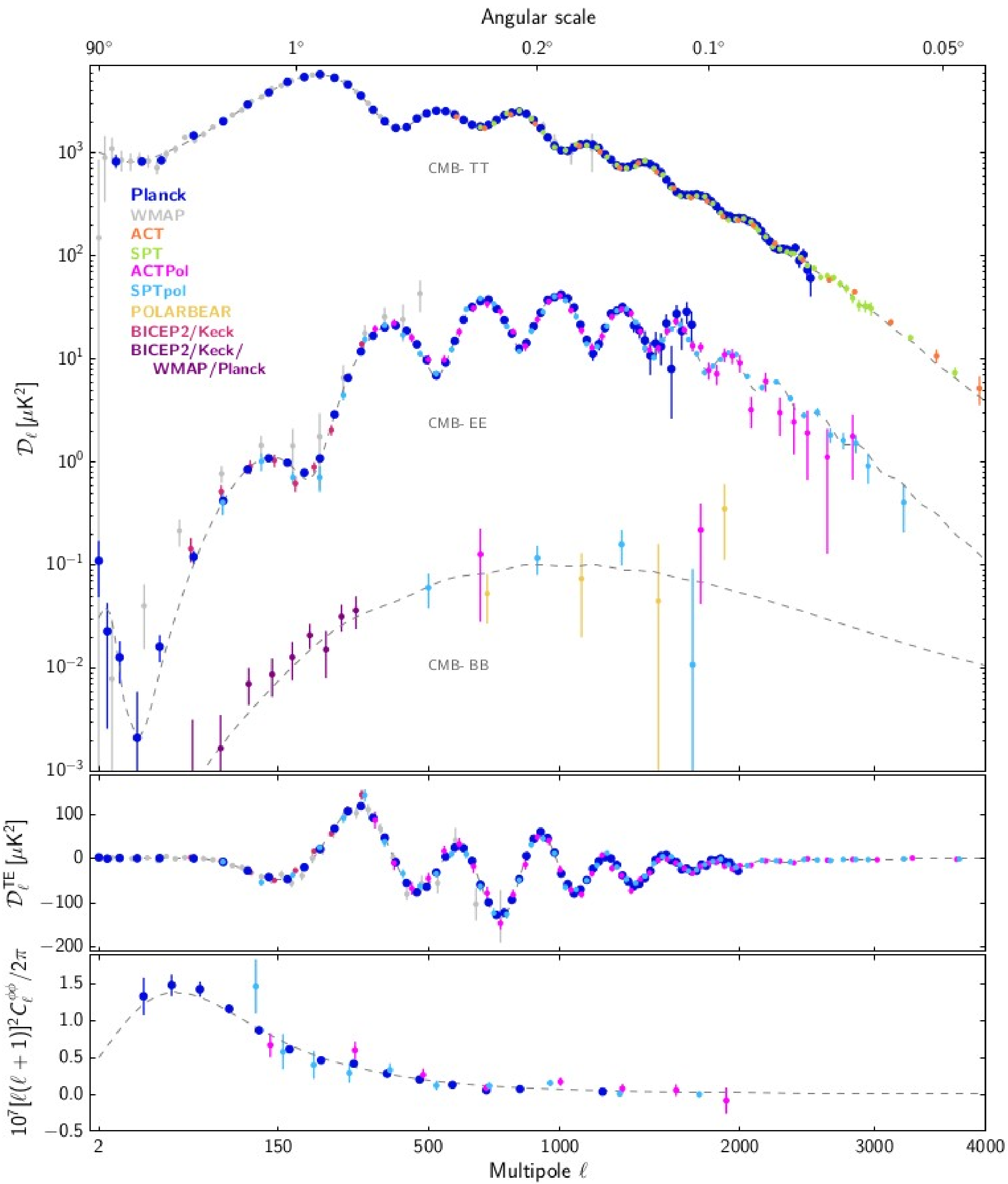
Angular scale
90°
1°
0.2°
0.1°
0.05°
CMB- TT
CMB- EE
CMB- BB
Planck
WMAP
ACT
SPT
ACTPol
SPTpol
POLARBEAR
BICEP2/Keck
BICEP2/Keck/
WMAP/Planck
$\mathcal{D}_\ell\,[\mu K^2]$
$\mathcal{D}_\ell^{TE}\,[\mu K^2]$
$10^7[\ell(\ell+1)]^2 C_\ell^{\phi\phi}/2\pi$
Multipole ℓ

Planck 2018

Planck 2018

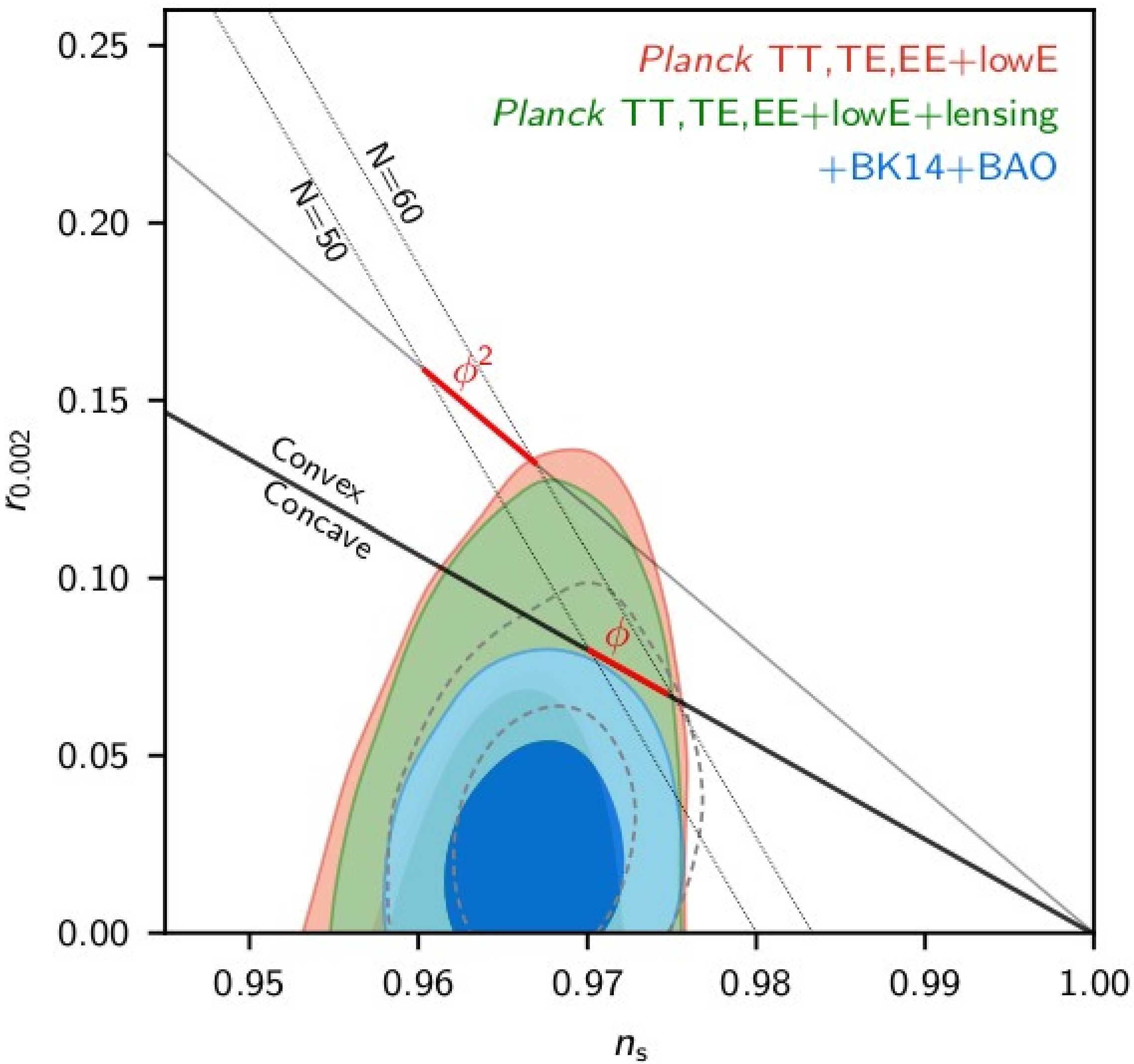

Planck TT,TE,EE+lowE
Planck TT,TE,EE+lowE+lensing
+BK14+BAO
N=50
N=60
Convex
Concave
ϕ^2
ϕ
$r_{0.002}$
n_s
0.25
0.20
0.15
0.10
0.05
0.00
0.95
0.96
0.97
0.98
0.99
1.00

Planck 2018

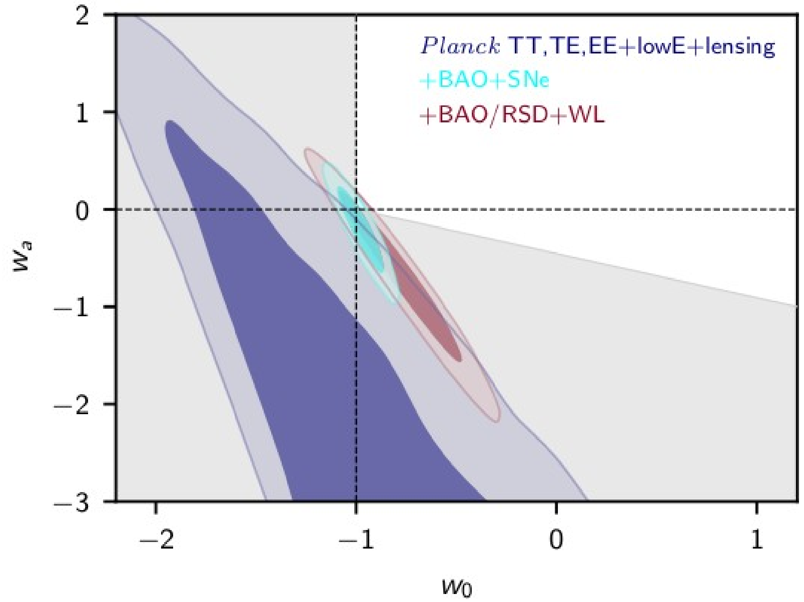

Planck TT,TE,EE+lowE+lensing
+BAO+SNe
+BAO/RSD+WL
w_a
w_0

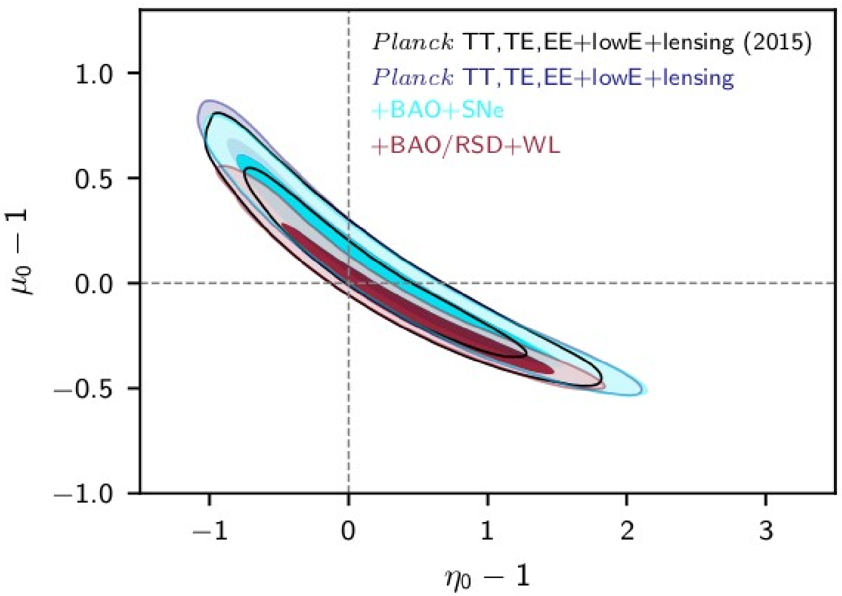

Planck TT,TE,EE+lowE+lensing (2015)
Planck TT,TE,EE+lowE+lensing
+BAO+SNe
+BAO/RSD+WL
$\mu_0 - 1$
$\eta_0 - 1$

Planck × BICEP × KECK 2018

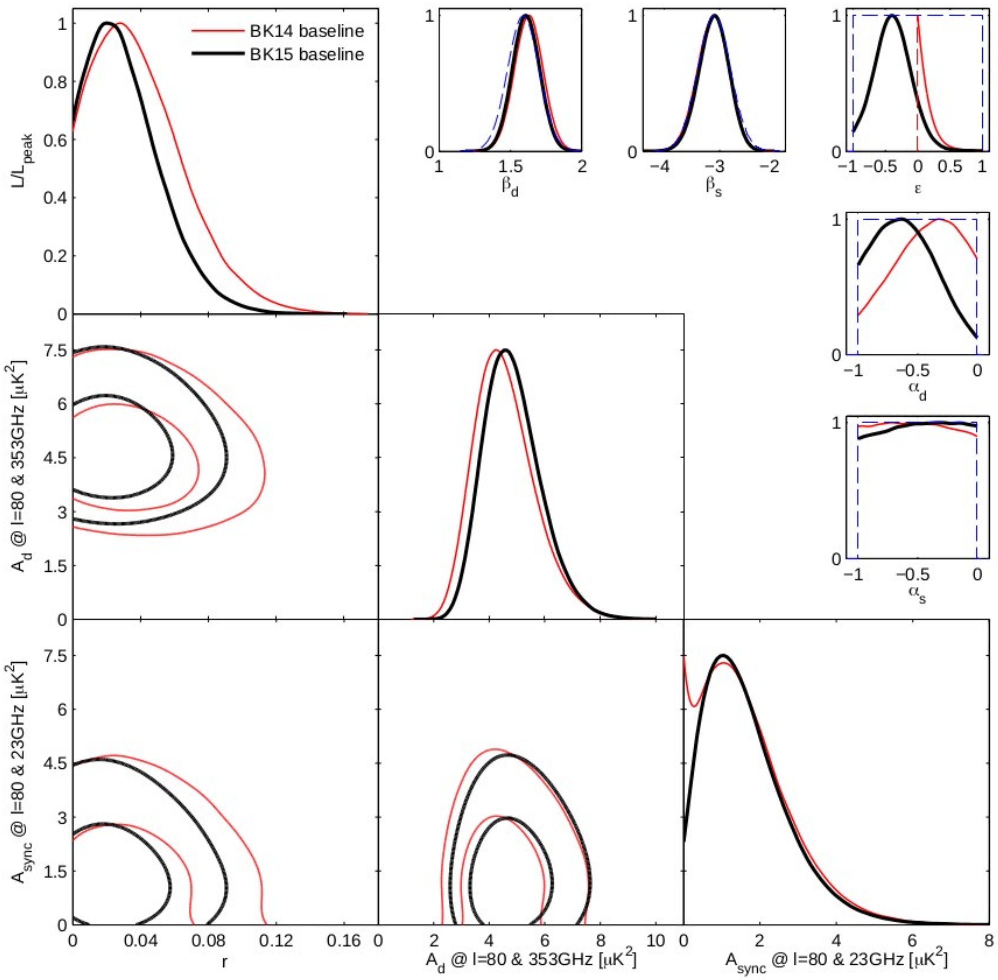

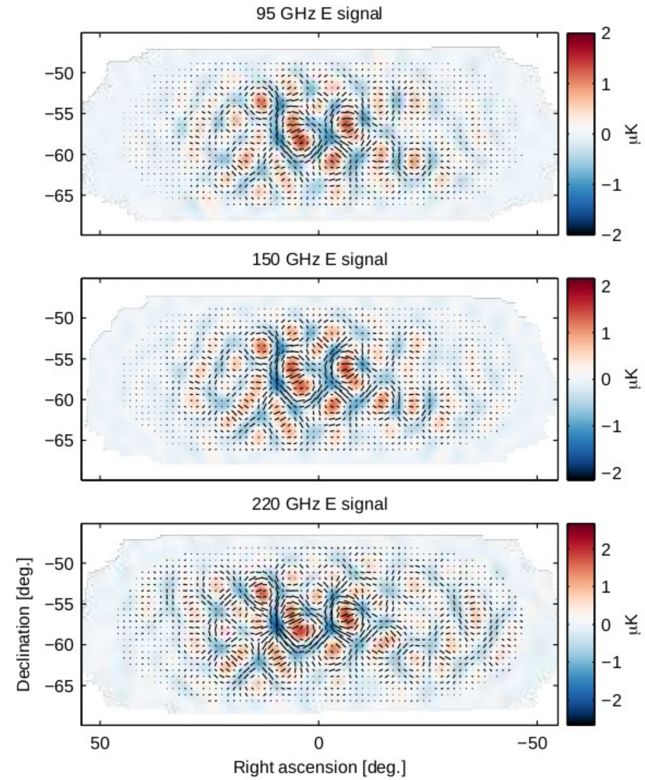

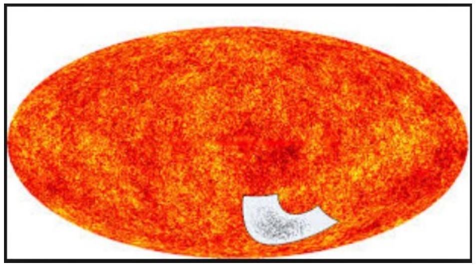

F=A (sky direction) × F(frequency)

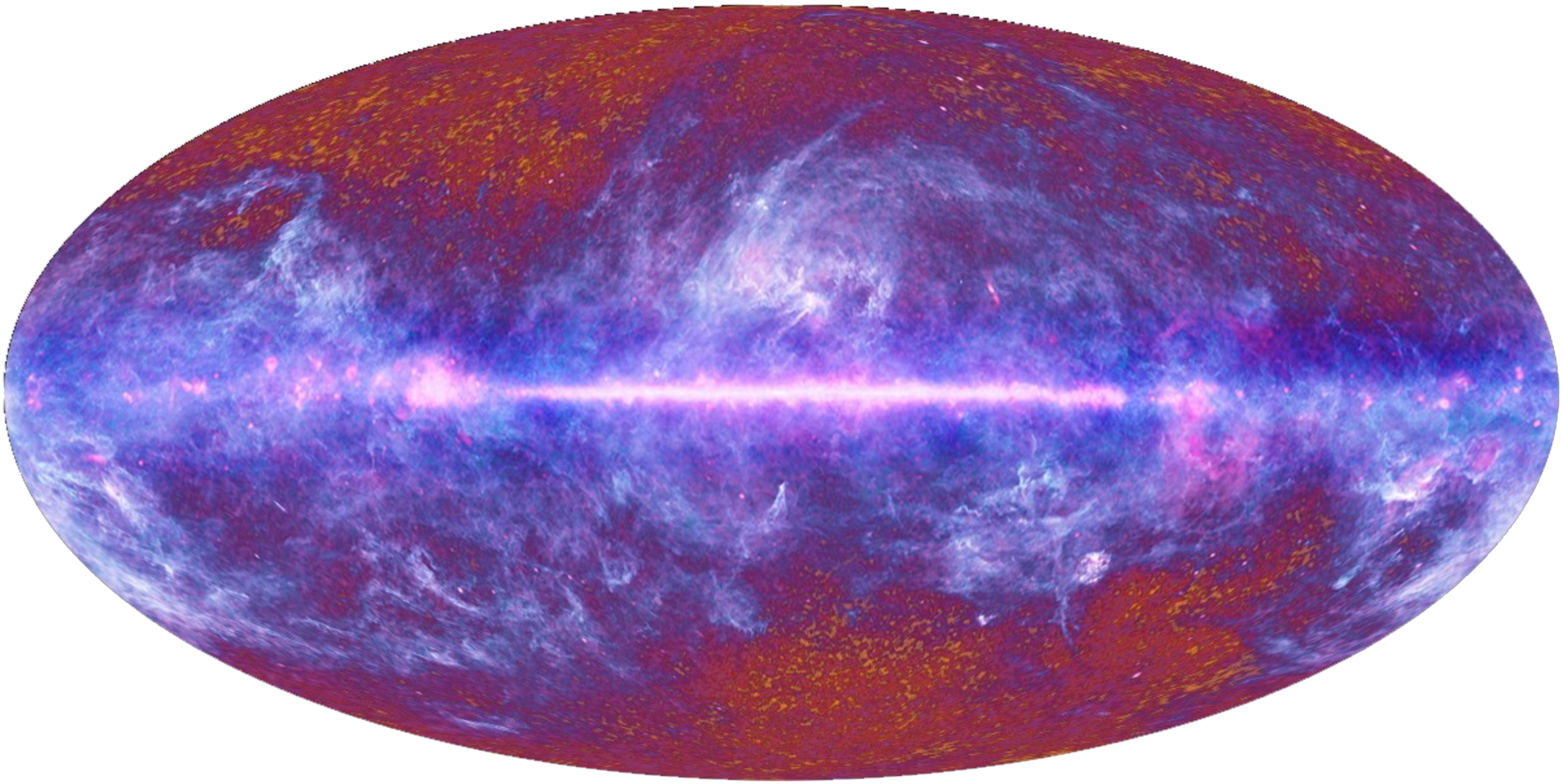

F=A (sky direction) × F(frequency)

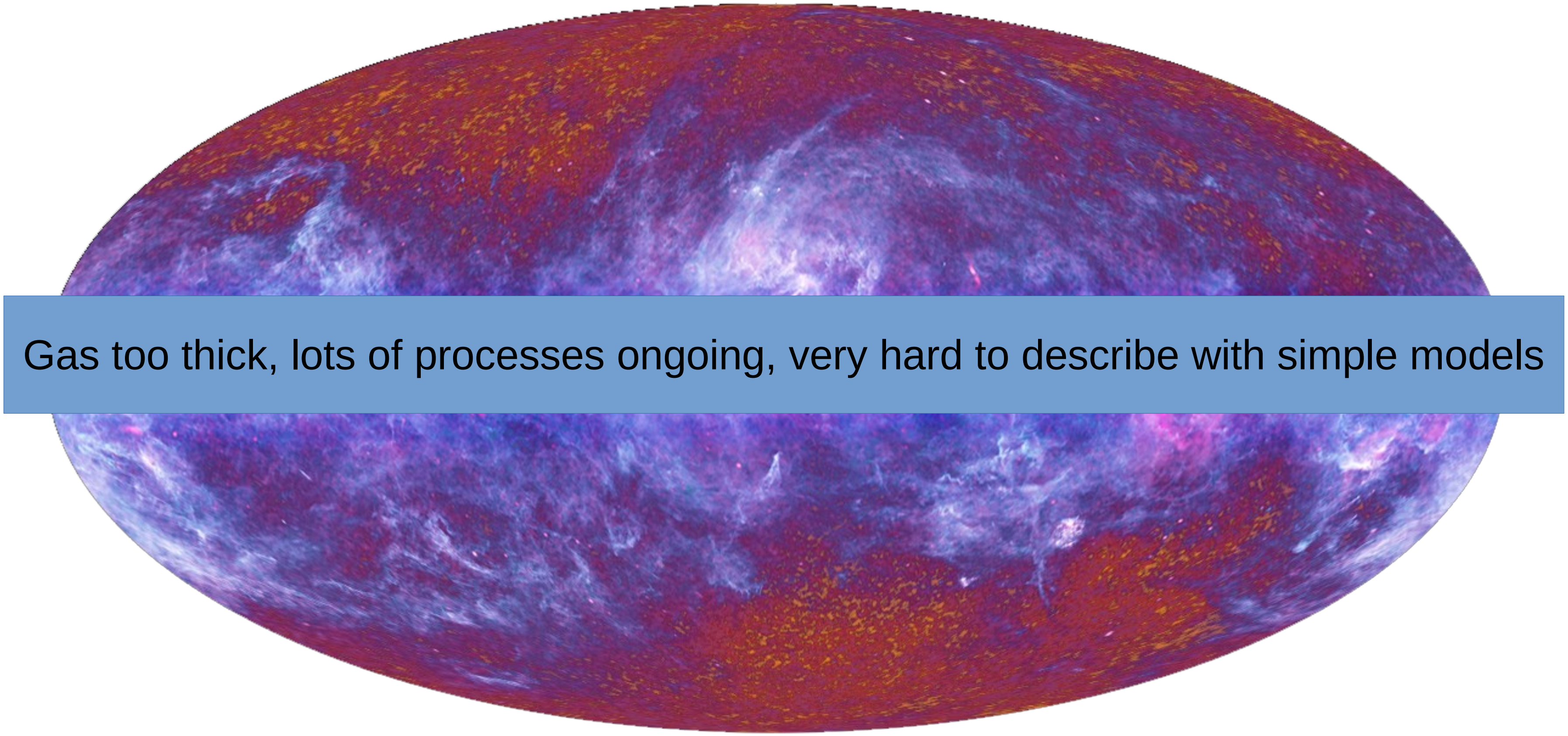

F=A (sky direction) × F(frequency)

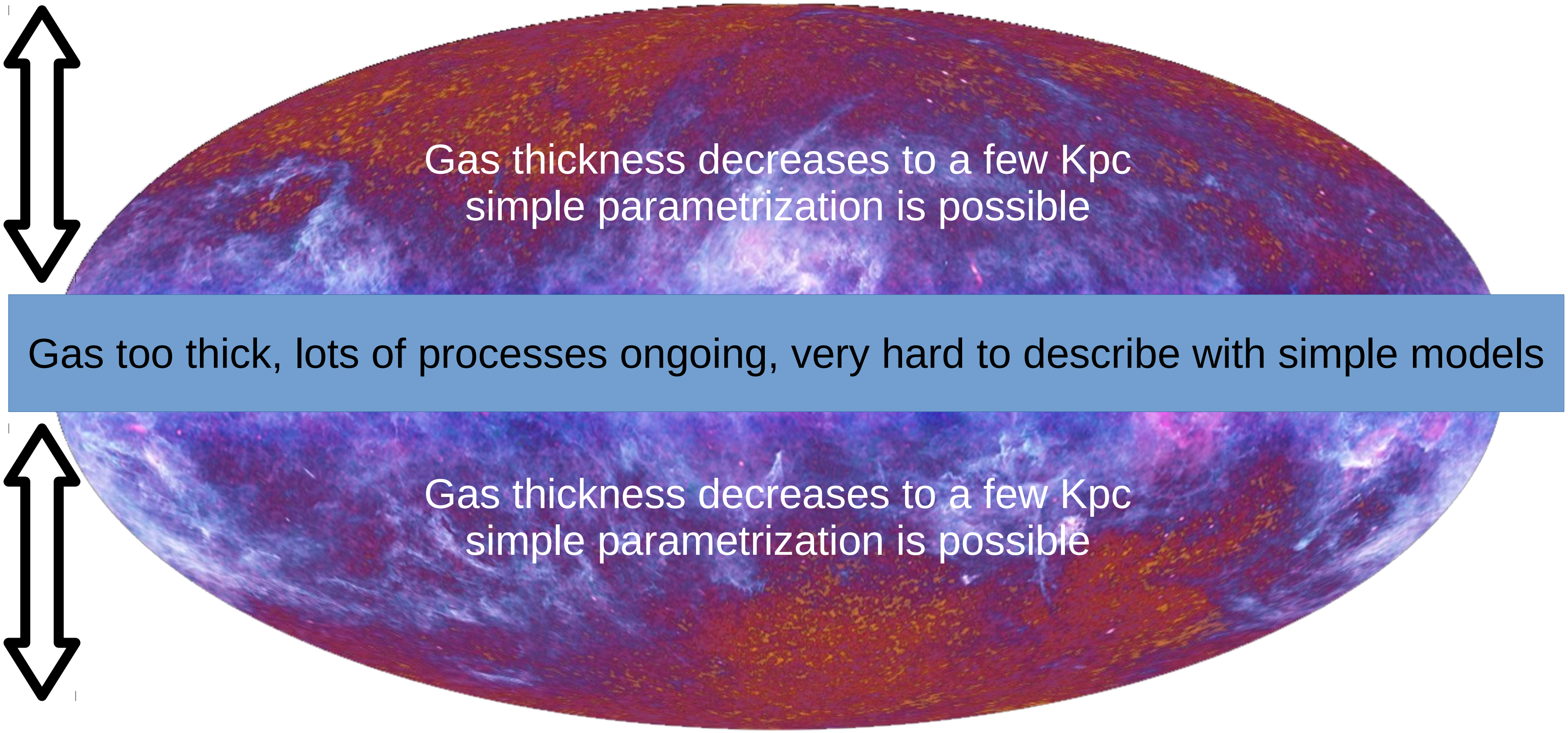

Planck 2013

Galactic polarized foregrounds

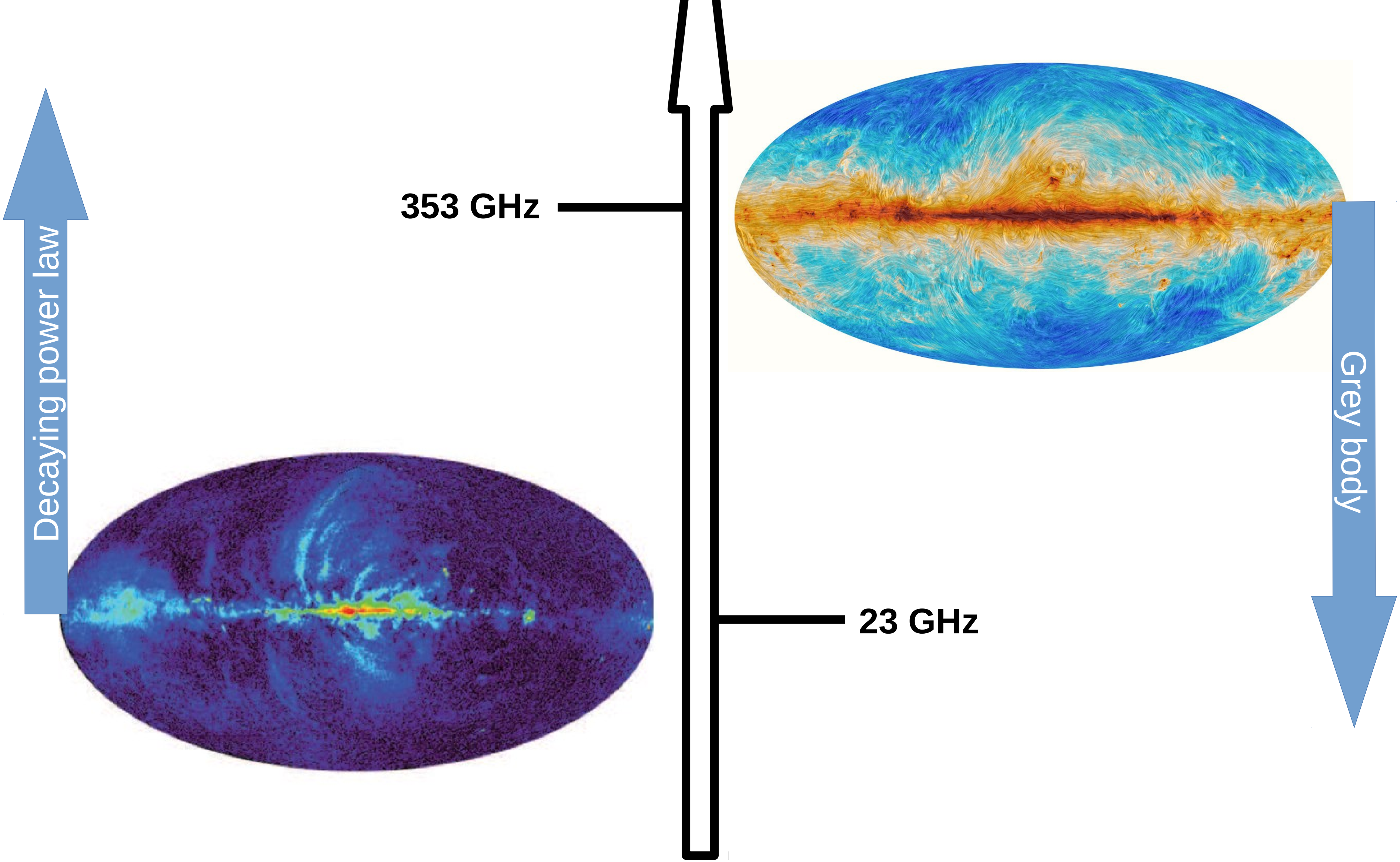

Polarized synchrotron

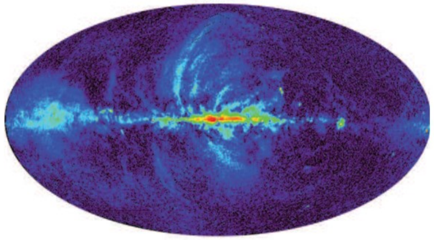

- Amplitude: cosmic ray electrons spilarizing around the Galactic magnetic field
- Frequency scaling: approximate decaying power law frequency scaling ($F_{RJ} \sim f^{-3}$), determined by the electron distribution in energy
- Data: total intensity and polarization, several surveys at radio frequencies, WMAP and Planck at microwave frequencies
- Data at the required quality for B-mode cleaning: none

Polarized dust

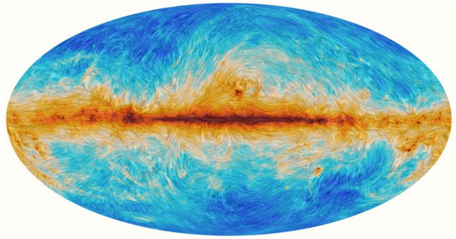

- Amplitude: magnetized dust grains emitting almost thermally, linearly polarized via local alignment with the Galactic magnetic field
- Frequency scaling: grey body $F_{RJ} \sim BB(f) \times f^{1.5}$
- Total intensity data: high resolution (few arcminutes) and sensitivity (IRAS and Planck) at 3000, 857, 545, 353 GHz for total intensity, degree scale mapping of temperature and emissivity
- Polarization data: Planck 2015 at 353 GHz
- Data at the required quality for B-mode cleaning: none

WMAP polarised foregrounds

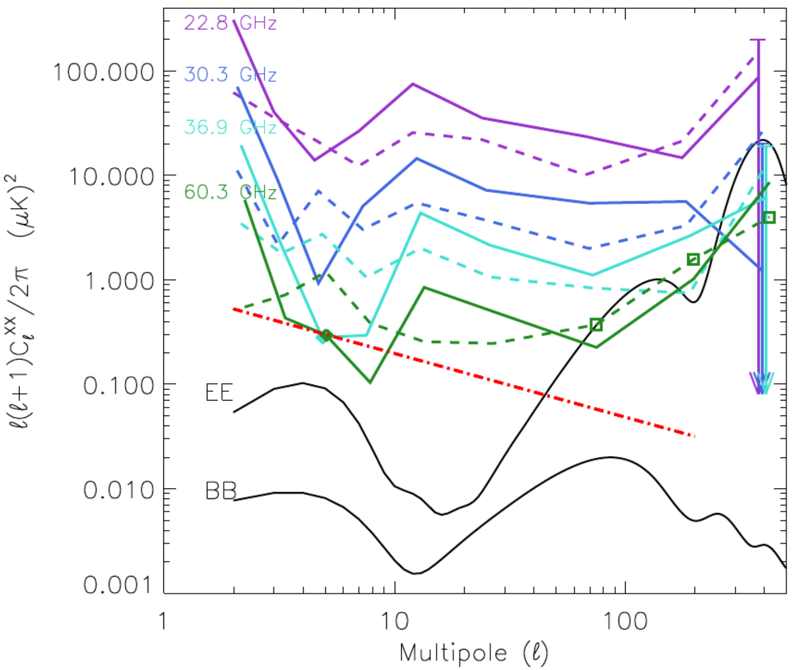

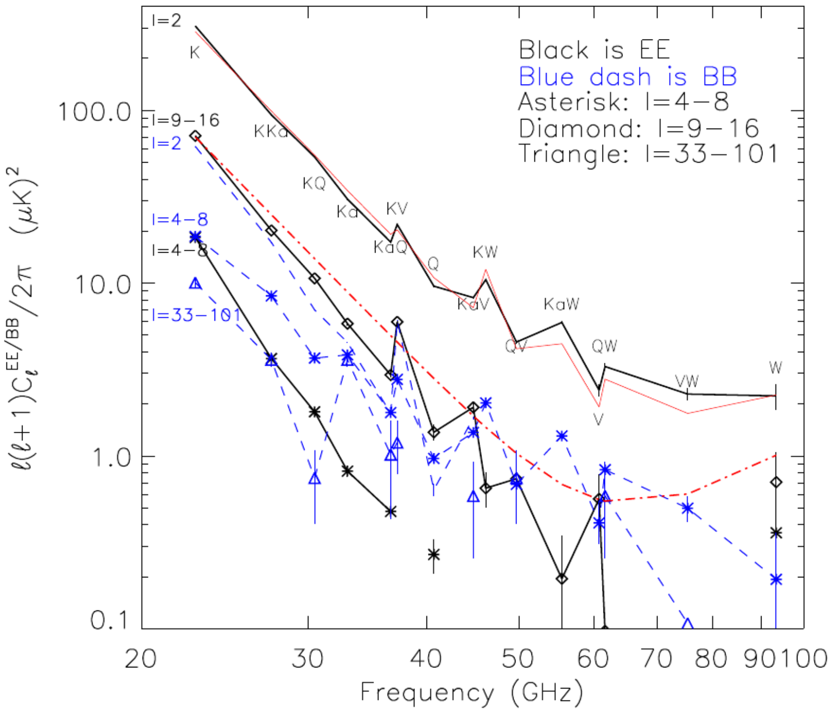

Page et al. 2007 for WMAP

Planck Sky Model

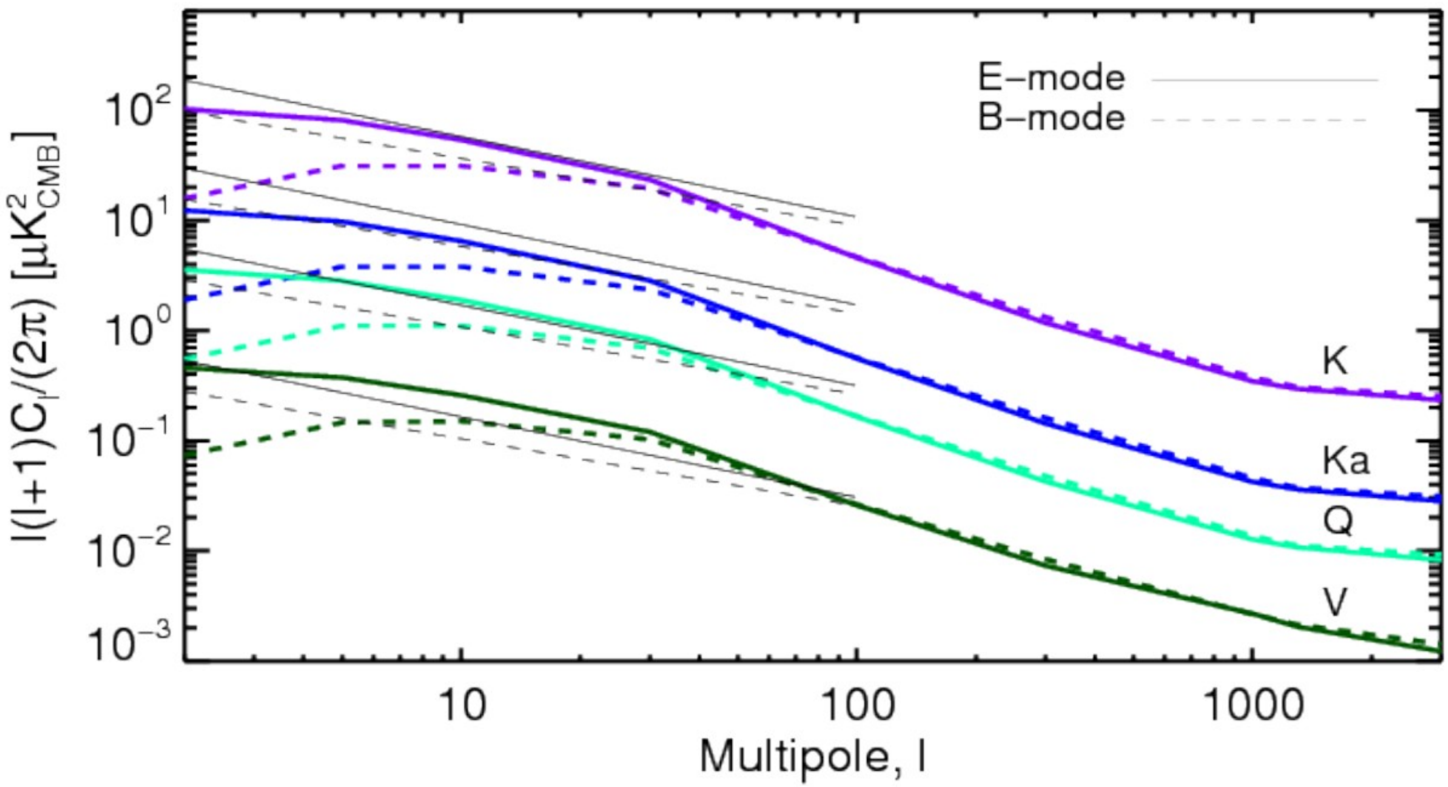

Delabrouille et al. 2012

Planck Sky Model

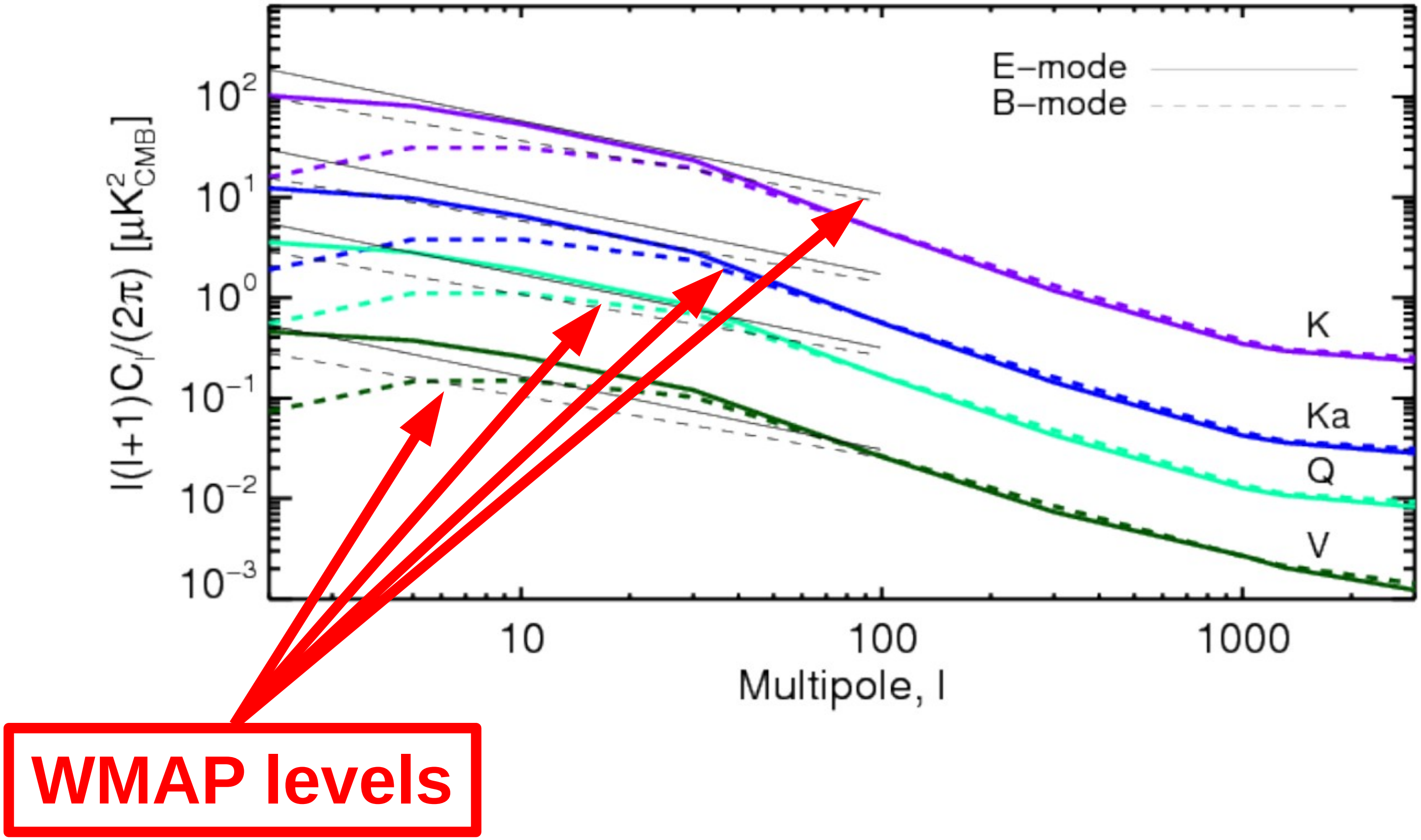

Delabrouille et al. 2012

Planck 2018: B-mode contamination

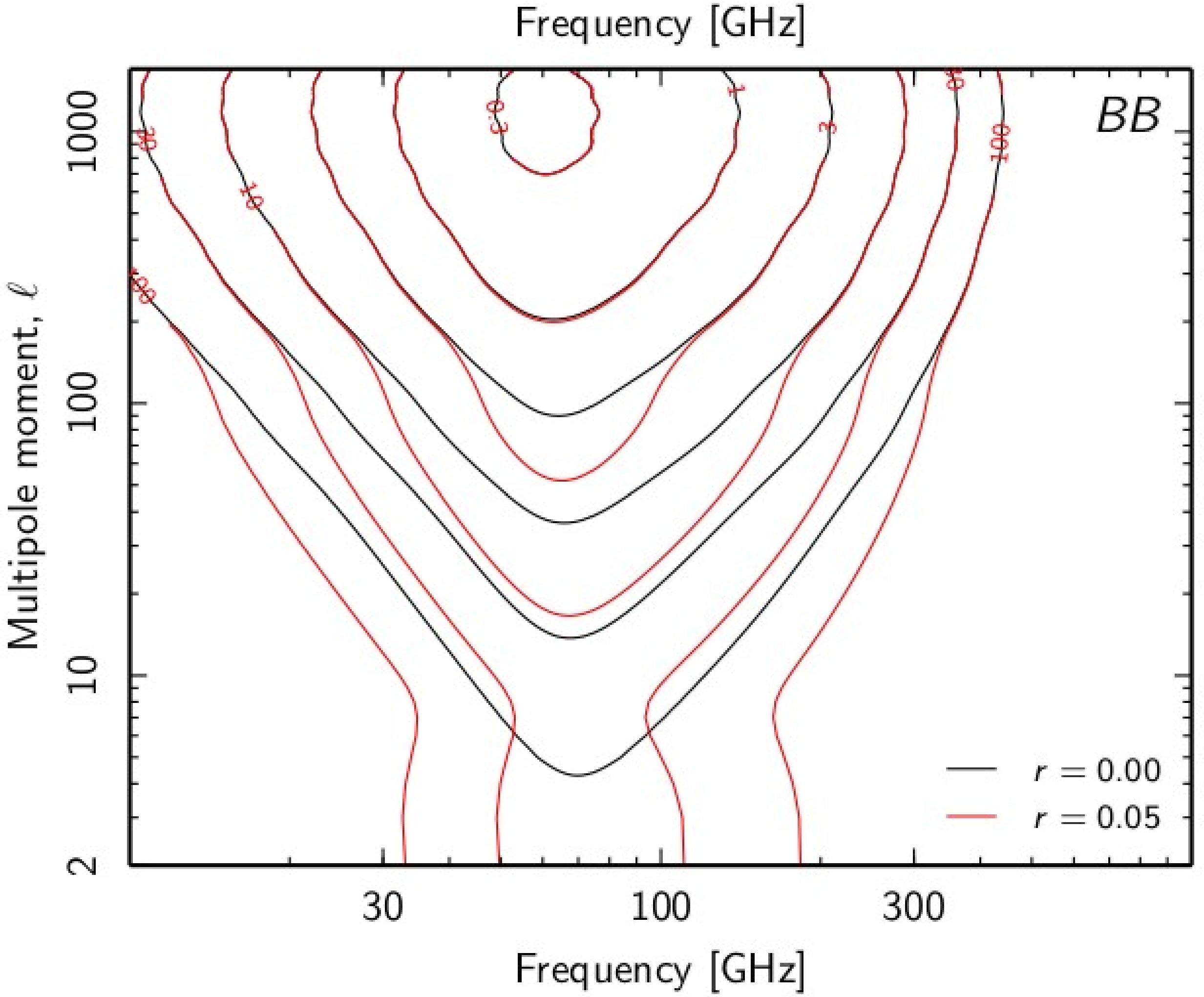

FG contamination to CMB B-modes

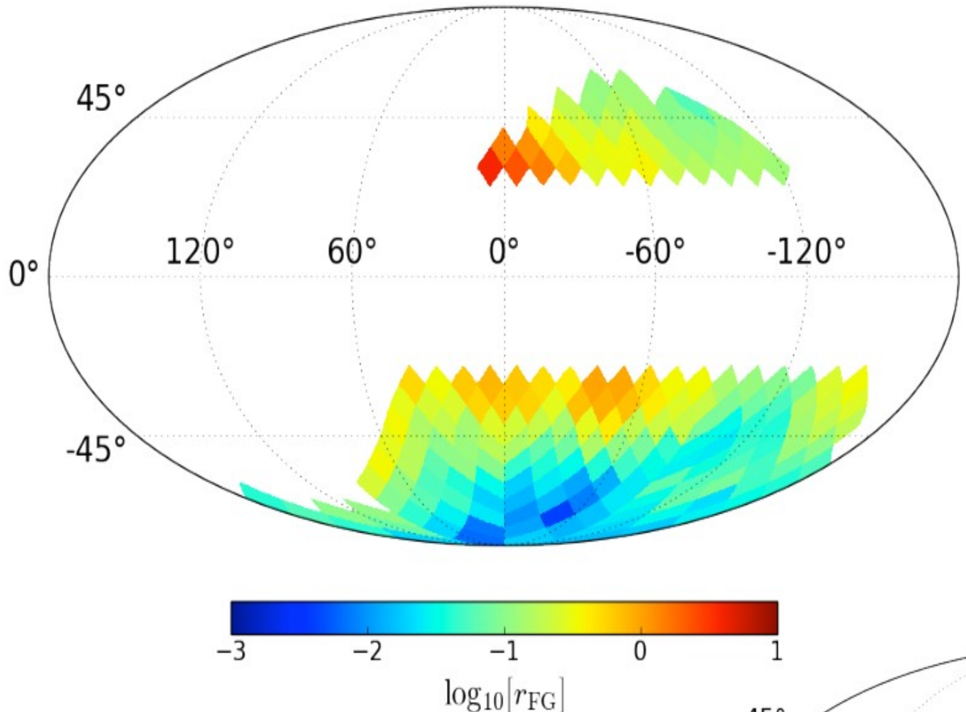

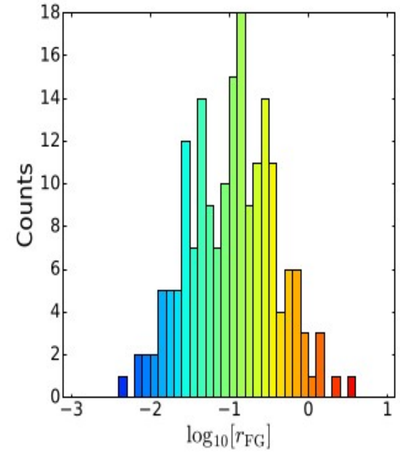

- **Foreground minumum** as sum of synch and dust amplitudes **at ℓ=80** neglecting correlation between the two

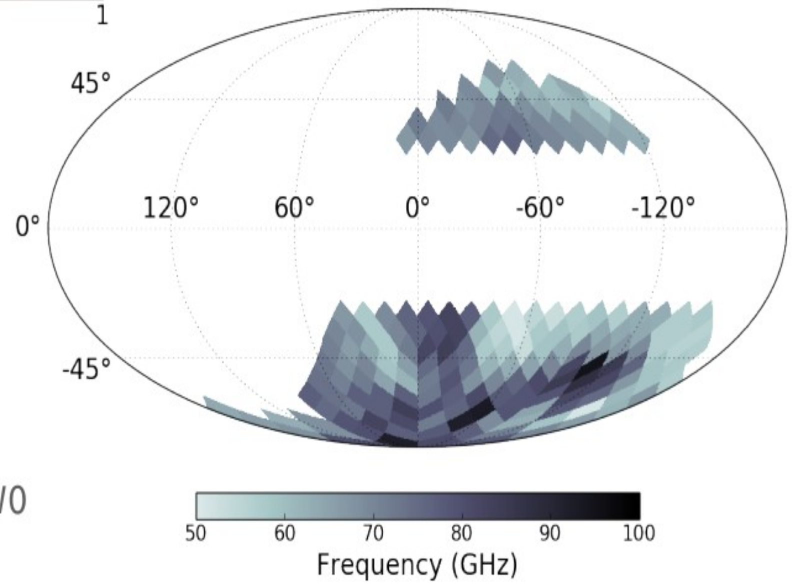

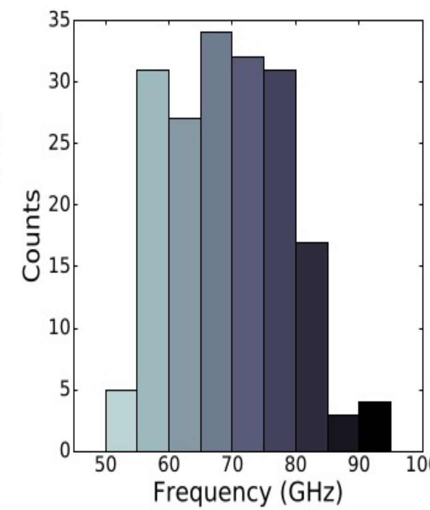

Krachmalnicoff et al. 2018

Planck × BICEP × KECK

$r < 0.07$ at 95% C.L.

BKP 2018

B-mode experiments in the next decade

A Moore's Law of CMB sensitivity

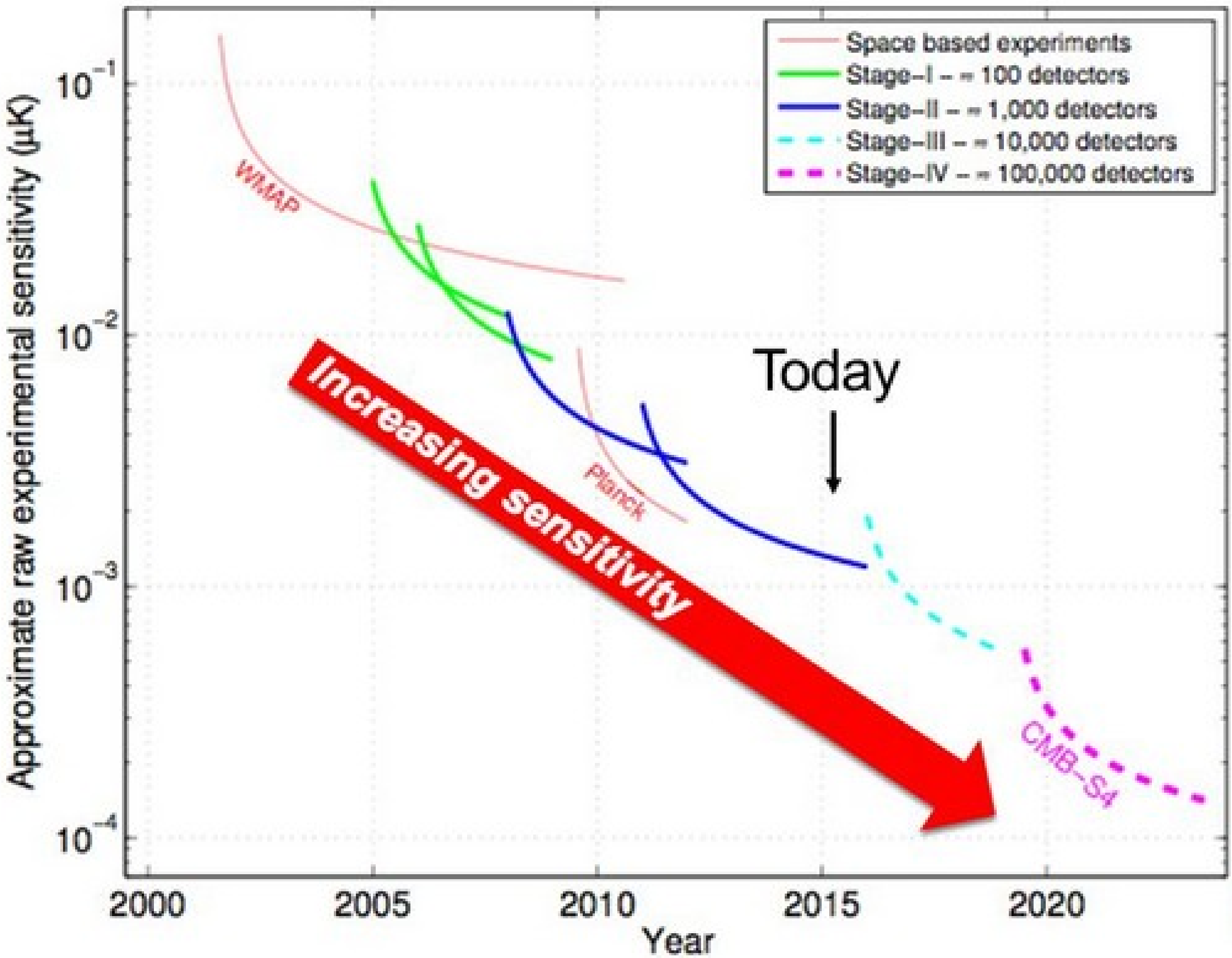

From Julian Borrill

Simons Array Projected Sensitivity

Multi-frequency
95, 150, 220, 270 GHz setup
Forecasts including
Foreground removal
10% sky fraction
3.5’ resolution at 150 GHz

$\sigma(r=0.1)=6\times10^{-3}$ (4×10^{-3} stat.)

$\sigma(\Sigma_\nu m_\nu)$=40 meV (19 meV stat.)

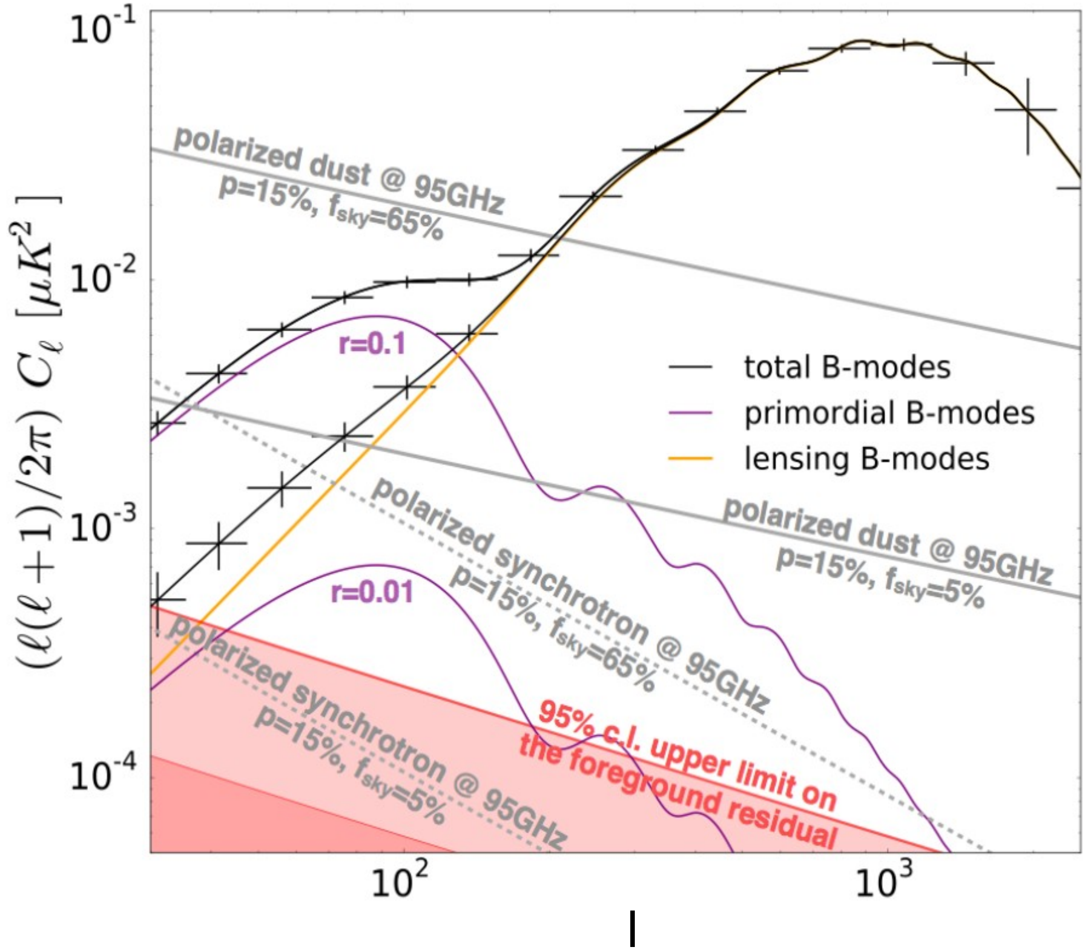

Plots by Josquin Errard

Simons Observatory

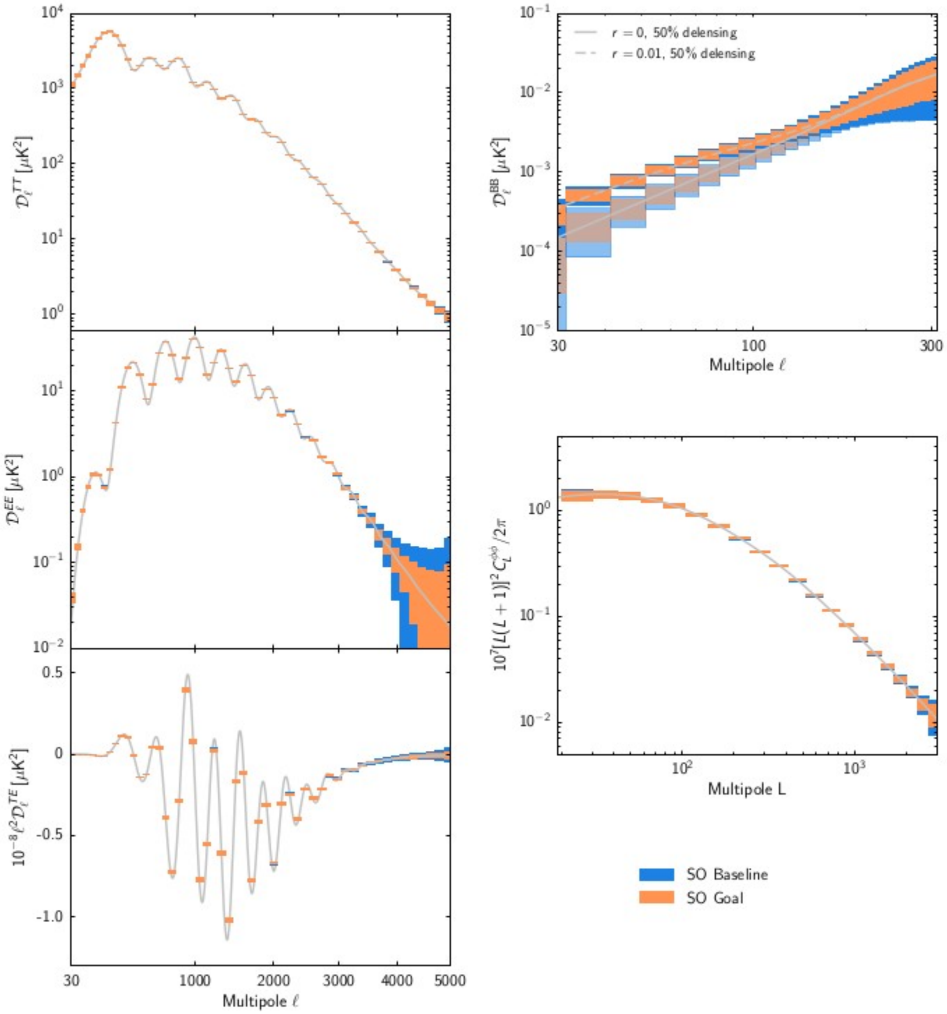

The Simons Observatory: Science Goals and Forecasts, arXiv:1808.07445

CMB-S4 Power Spectra

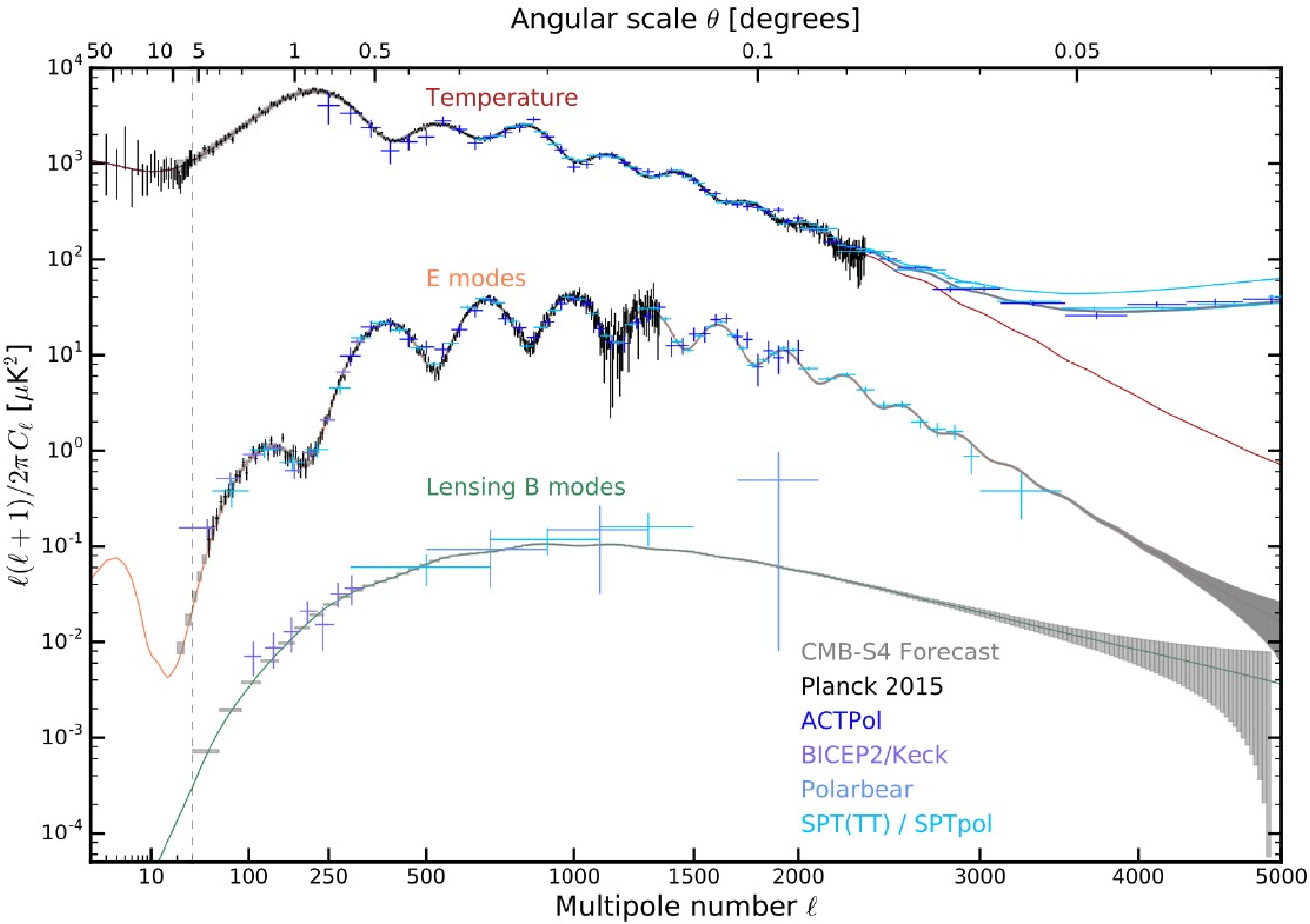

CMB-S4 Science Book: arxiv:1610.02743

COSMOS
Cosmic Orbital and Suborbital Microwave ObservationS

LiteBIRD

Detector array sensitivity (NET_{arr})

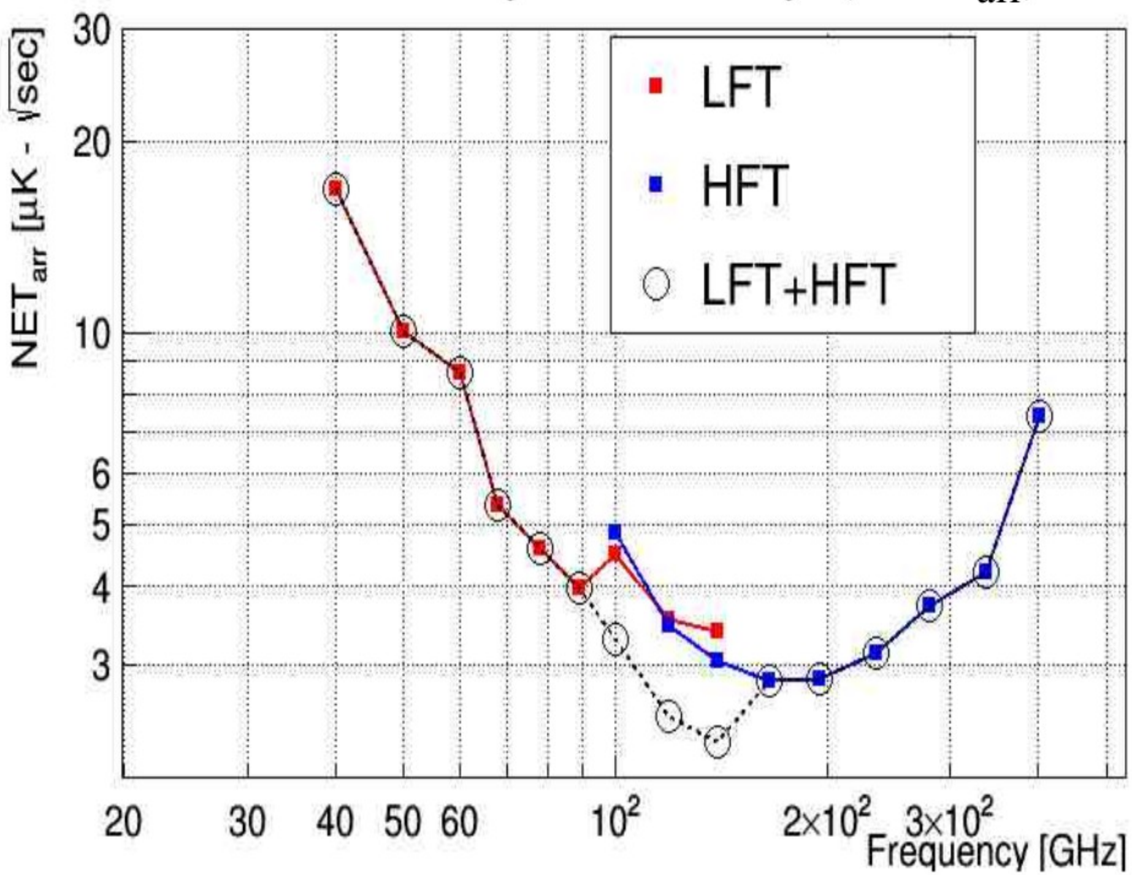

NET_{arr} → Sky sensitivity

Frequency [GHz]	$NET_{CMB,Arr}$ [$\mu K \cdot \sqrt{s}$]	Sensitivity [μK – arcmin]
40	16.76	34.99
50	10.04	20.96
60	8.67	18.09
68	5.37	11.21
78	4.57	9.54
89	3.97	8.29
100	3.39	6.88
119	2.49	5.19
140	2.27	4.75
166	2.85	5.96
195	2.86	5.97
235	3.13	6.52
280	3.73	7.79
337	4.22	8.82
402	7.40	15.44

(3yr obs.)

JAXA
NASA
ESA Design Study & European Consortium
ASI, CNES supporting Phase A

$\delta r < 1 \times 10^{-3}$

From Masashi Hazumi

B-mode power spectrum measurements

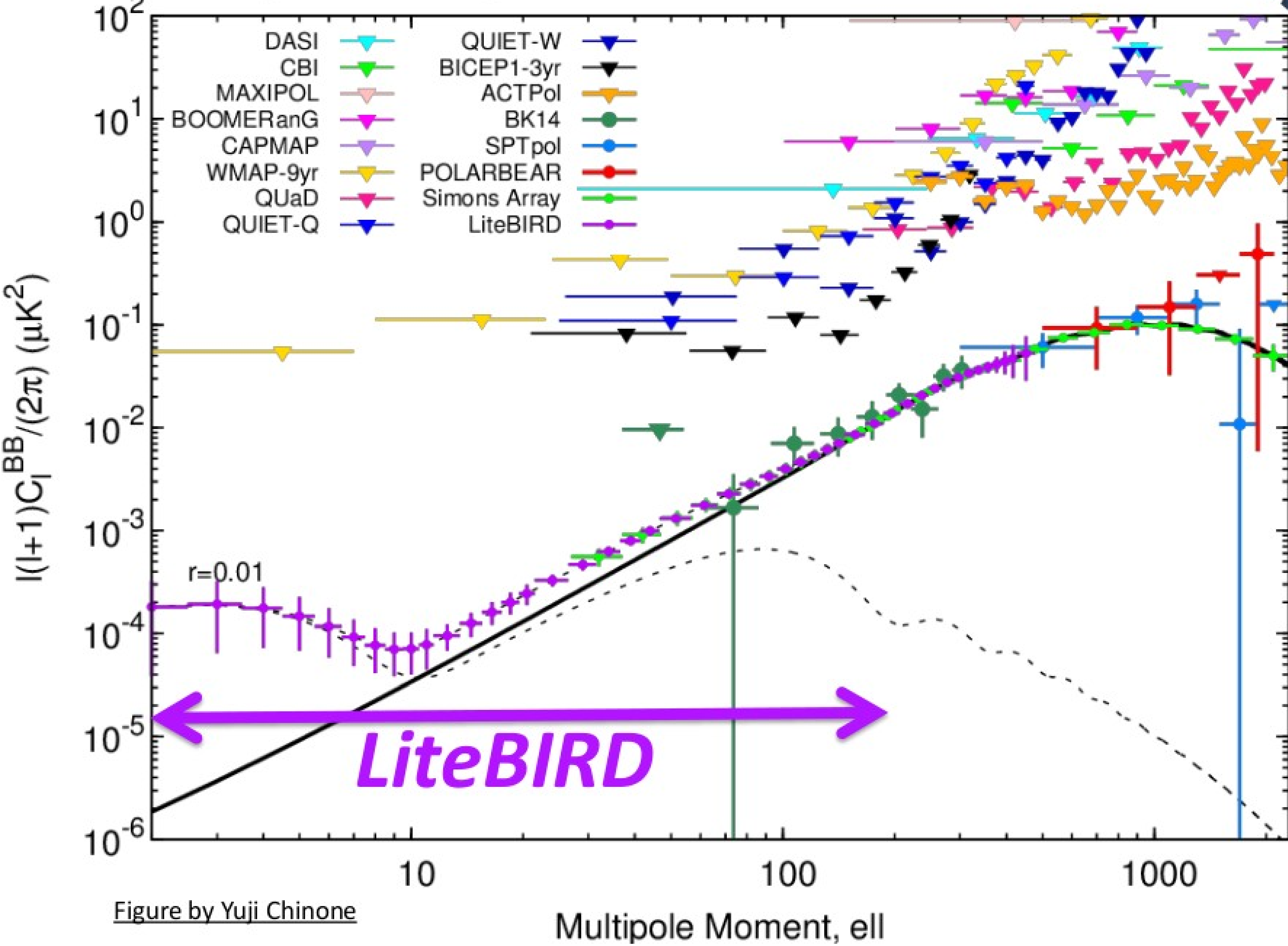

Figure by Yuji Chinone

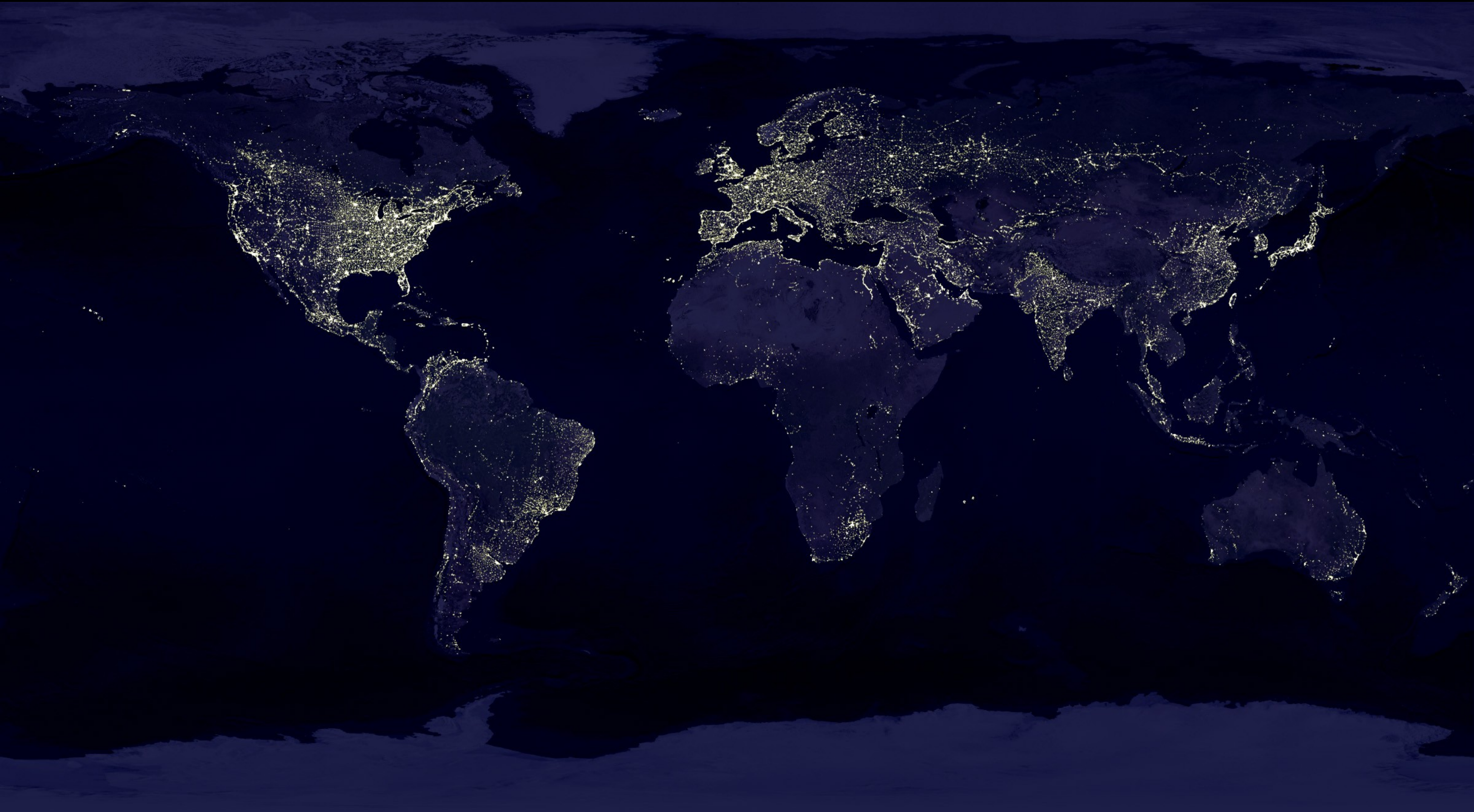

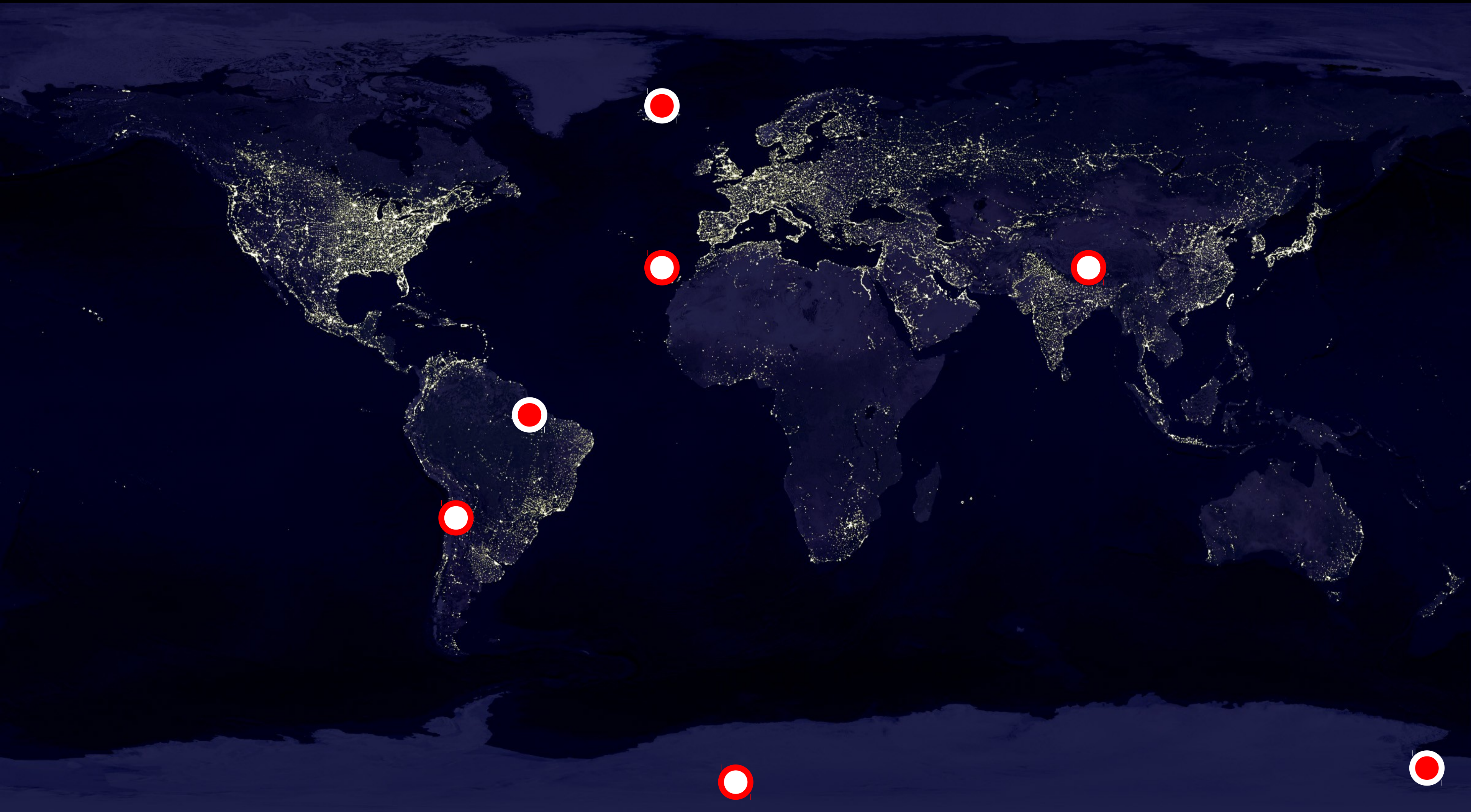

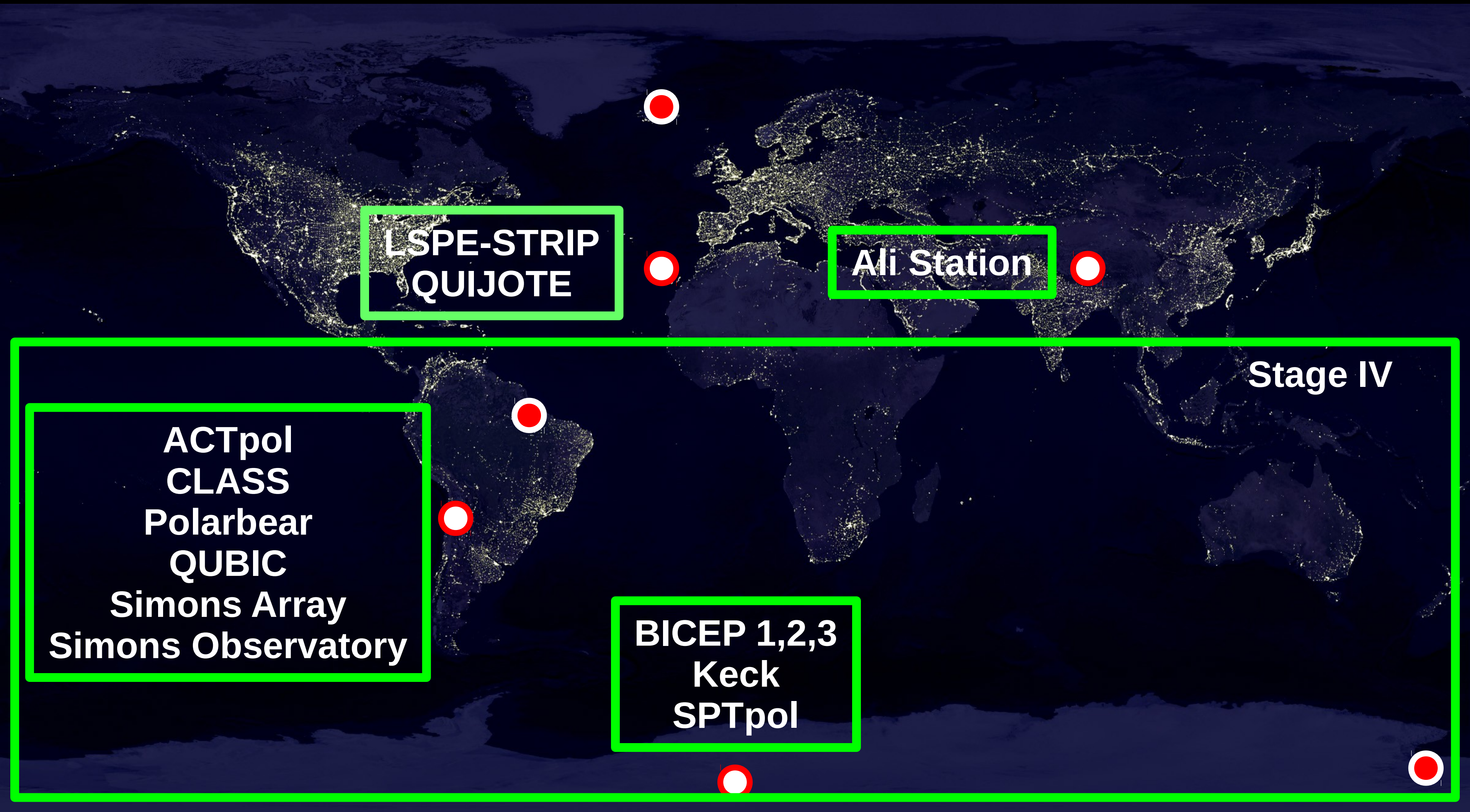
LSPE-STRIP
QUIJOTE
Ali Station
Stage IV
ACTpol
CLASS
Polarbear
QUBIC
Simons Array
Simons Observatory
BICEP 1,2,3
Keck
SPTpol

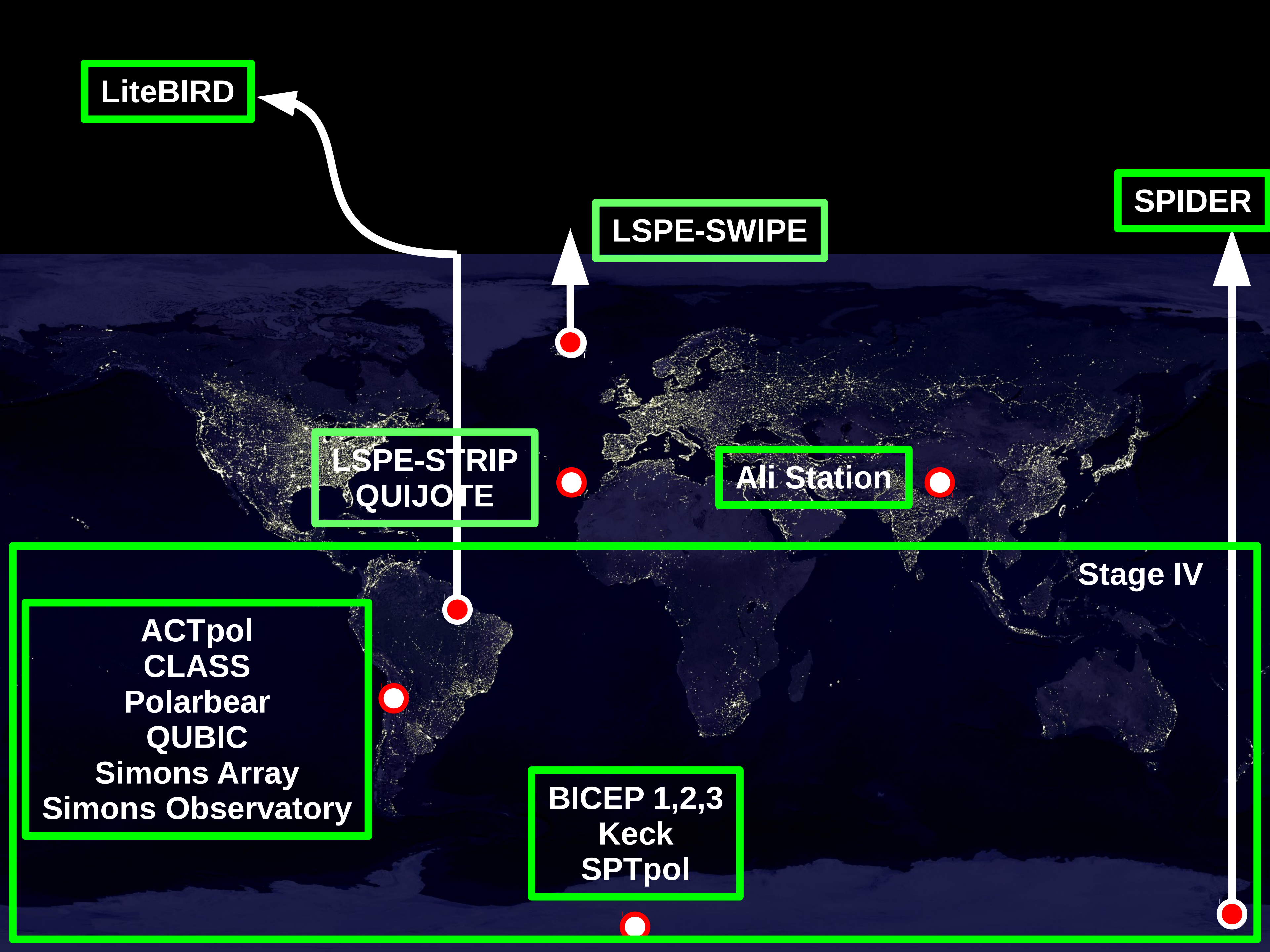
LiteBIRD
LSPE-SWIPE
SPIDER
LSPE-STRIP
QUIJOTE
Ali Station
Stage IV
ACTpol
CLASS
Polarbear
QUBIC
Simons Array
Simons Observatory
BICEP 1,2,3
Keck
SPTpol

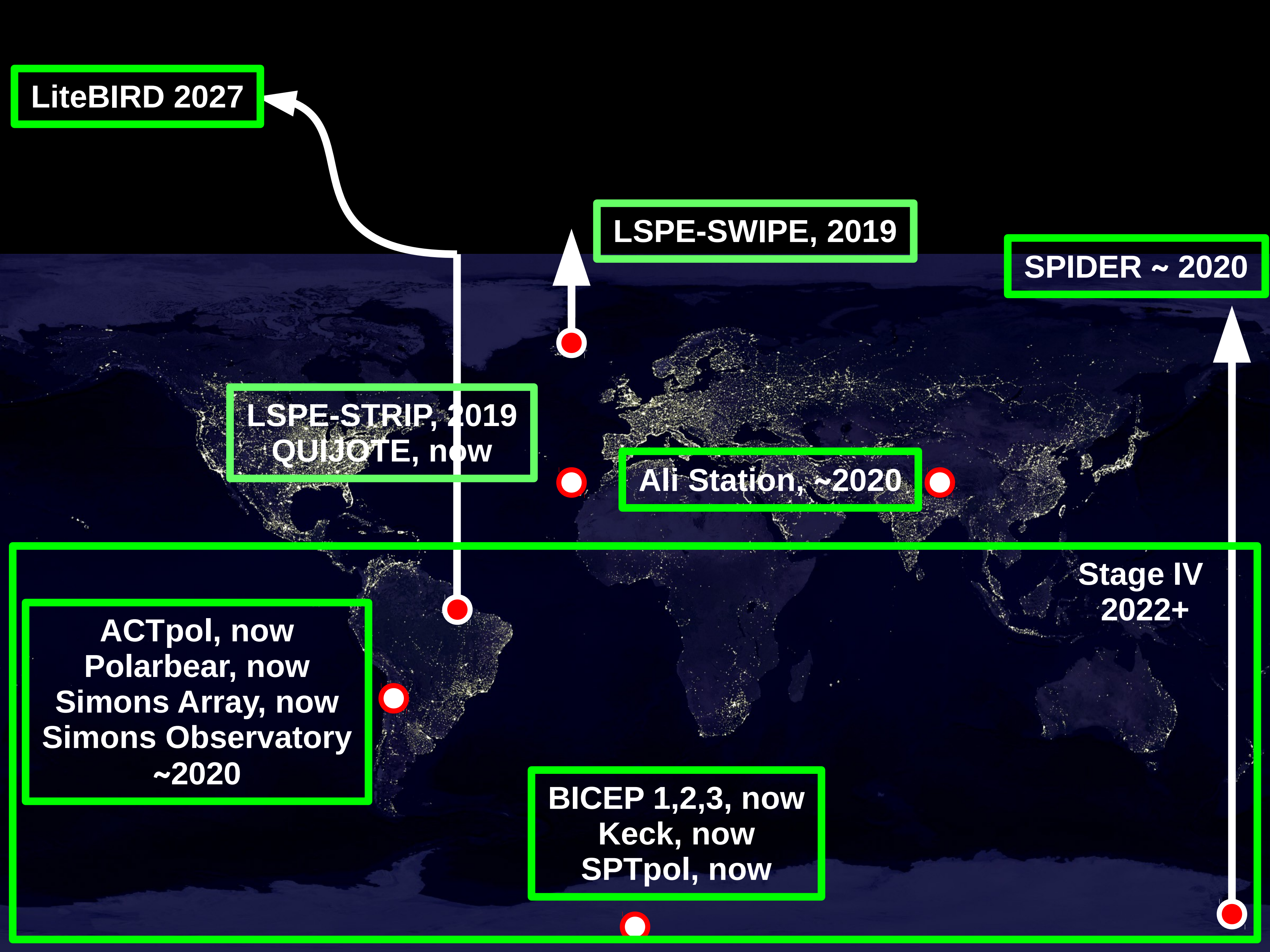
LiteBIRD 2027
LSPE-SWIPE, 2019
SPIDER ~ 2020
LSPE-STRIP, 2019
QUIJOTE, now
Ali Station, ~2020
Stage IV
2022+
ACTpol, now
Polarbear, now
Simons Array, now
Simons Observatory
~2020
BICEP 1,2,3, now
Keck, now
SPTpol, now